Persoonia 41, 2018: 109–129
www.ingentaconnect.com/content/nhn/pimj

RESEARCH ARTICLE

ISSN (Online) 1878-9080
https://doi.org/10.3767/persoonia.2018.41.06

Removing chaos from confusion: assigning names to common human and animal pathogens in *Neocosmospora*

M. Sandoval-Denis[1,2], P.W. Crous[1,2]

Key words

eight new taxa
Fusarium
Neocosmospora
pathogens
phylogeny
systematics

Abstract The genus *Neocosmospora* encompasses highly prevalent and aggressive human and animal fungal pathogens. Here we assign formal descriptions and Latin binomials to some of the most clinically relevant phylogenetic species of the genus. Three new species, named *Neocosmospora catenata*, *N. gamsii* and *N. suttoniana* (previously assigned to the informal names '*Fusarium*' *solani* species complex (FSSC) lineages, FSSC 43, FSSC 7 and FSSC 20, respectively) are described on the basis of multilocus phylogenetic analyses (using *EF-1α*, ITS, LSU and *RPB2* loci) and morphological characters. Lineage FSSC 9 is conspecific with the ex-type strain of *Cylindrocarpon tonkinense*, thus the new combination *Neocosmospora tonkinensis* is proposed. In addition, and based on the latest taxonomy for this generic complex, new combinations are introduced for four medically important taxa: *Neocosmospora keratoplastica*, *N. lichenicola*, *N. metavorans* and *N. petroliphila*. The most significant distinctive features for all the clinically relevant species treated here are compared and illustrated.

Article info Received: 27 August 2017; Accepted: 30 November 2017; Published: 4 April 2018.

INTRODUCTION

The genus *Neocosmospora* (as the '*Fusarium*' *solani* species complex, FSSC) has been a highly renowned fungal group for more than 100 years, mainly because it contains significant plant pathogenic species, including agents of fruit-rot, root-rot and seedling damping-off, affecting diverse plant hosts (Leslie & Summerell 2006, Domsch et al. 2007, Nalim et al. 2011). In the last 50 years, however, this fungal group gradually and persistently became recognised as important in the clinical field. It is now known to contain some of the fungal species that are most clinically relevant as agents infecting immunocompetent hosts. This list of species includes the principal etiologic agents of fungal keratitis, which are often introduced via traumatic inoculation (De Hoog et al. 2000, Godoy et al. 2004, Shukla et al. 2008). In addition are the second most commonly isolated moulds in onychomycosis after the dermatophytes (Ghannoum et al. 2000, Scher et al. 2013). Species in *Neocosmospora* are also among the most significant pathogens associated with severe infections in transplant recipients and patients with haematological malignancies, persistent neutropenia or immunodepression caused by corticosteroid therapy (Lass-Flörl 2009, Torres & Kontoyiannis 2011, Guarro 2013, Slavin et al. 2015). Although fusarial infections are rare, nearly 50 % of these infections are attributed to *Neocosmospora*. The most commonly reported species correspond to '*F.' keratoplasticum*, '*F.' petroliphilum*, *N. falciformis* (syn. *F. falciforme*) and *N. solani* (syn. *F. solani*); plus several currently unnamed phylogenetic species. These organisms are recovered from diverse cutaneous and subcutaneous infections including arthritis, brain abscess, catheter-associated fungemia, disseminated infections, mycetoma, osteomyelitis, peritoneal dialysis-associated peritonitis and sinusitis, as well as many other types of infections (Dignani & Anaissie 2004, Garcia et al. 2015, Hiebert et al. 2016).

Human pathogenic species in *Neocosmospora* are also among the most important fusarial agents of veterinary infections (Zhang et al. 2006, O'Donnell et al. 2008, 2010, 2016). Apart from *N. solani*, other species seem to show some degree of host specialisation. *Neocosmospora falciformis* has been repeatedly isolated from equine ocular infections, and has also been reported from canines and reptiles (O'Donnell et al. 2016), while '*F'. keratoplasticum* and two currently unnamed phylogenetic species (FSSC 12 and FSSC 43) seem to have some adaptation to the marine environment, infecting mostly crustaceans, fish, marine mammals and reptiles (O'Donnell et al. 2016).

The generally high degree of antifungal resistance, variable *in vitro* susceptibility patterns and unpredictable response to antifungal compounds seen in *Neocosmospora* infections, coupled with the high virulence described in clinical reports and animal models of infection, are factors often associated with negative outcomes, placing these species among the most devastating fungal agents of human and animal disease (Sugiura et al. 2003, Azor et al. 2007, Araujo et al. 2015, Espinel-Ingroff et al. 2016, Taj-Aldeen et al. 2016).

Phylogenetic studies have shown that *Neocosmospora solani*, historically linked with human and veterinary disease, do not belong to a discrete taxon but rather represent an extensive evolutionary radiation comprising more than 15 phylogenetic species. With the exception of the four most commonly isolated species, *N. falciformis*, '*F.' keratoplasticum*, '*F.' petroliphilum* and *N. solani*, most of these phylospecies have not been formally described, thus are not linked to scientific names, in part because they are scarcely distinguishable by means of phenotypic comparison. Although phylogenetically well characterised, comprehensive morphological descriptions and diagnoses do not exist for these important lineages, which are currently identified following an informal haplotype nomenclatural system (Zhang et al. 2006, O'Donnell et al. 2008).

[1] Westerdijk Fungal Biodiversity Institute, Uppsalalaan 8, 3584 CT Utrecht, The Netherlands;
corresponding author e-mail: m.sandoval@westerdijkinstitute.nl.
[2] Faculty of Natural and Agricultural Sciences, Department of Plant Sciences, University of the Free State, P.O. Box 339, Bloemfontein 9300, South Africa.

The use of Latin binomials is not a common feature for clades containing human and veterinary pathogens in *Neocosmospora*, mainly due to the conflicting taxonomy of the genus, the non-existence of nomenclatural types and the uncertainty of application of previously published names. Moreover, the name '*Fusarium' solani* has been traditionally used by clinical microbiologists and plant pathologists as a wildcard to deal with isolates belonging to this complex when molecular tools are not available (Zhang et al. 2006, Nakamura et al. 2007, Bachmeyer 2007, O'Donnell et al. 2016). Meanwhile, new lineages not conforming to an existing haplotype designation are constantly being found (Guevara-Suarez et al. 2016, Melo et al. 2016).

Recently, Schroers et al. (2016) epitypified *Neocosmospora solani* (basionym: *Fusisporium solani*) linking this important plant and animal pathogen with clade 5 in FSSC. Al-Hatmi et al. (2018) formally proposed the name '*Fusarium' metavorans* for FSSC 6, one of the most prevalent lineages in human disease, while FSSC 12, which includes important veterinary pathogens, is currently under study and will soon be formally described (Geiser pers. comm.). However, several unnamed clades are still in need of formal description, and those containing animal pathogens are of particular importance (O'Donnell et al. 2008, 2016). An accurate identification of pathogenic fusaria is essential for epidemiological purposes and for the prompt establishment of efficacious clinical treatment (Bachmeyer 2007). It is known that antifungal susceptibility in fusaria is variable among closely related taxa, and often isolate-dependant (Alastruey-Izquierdo et al. 2008, Tortorano et al. 2008). This phenomenon has not yet been reported in *Neocosmospora* (Azor et al. 2007, Bachmeyer 2007), and remains an understudied issue in the genus.

In the present study, we examine a set of isolates previously assigned to five of the most prevalent pathogenic clades in *Neocosmospora* (*'F.' metavorans*, FSSC 7, FSSC 9, FSSC 20 and FSSC 43), along with strains belonging to the most commonly encountered clinically relevant species mentioned above. Latin binomials, detailed illustrations, morphological descriptions and comparisons are provided in order to facilitate identification by clinical microbiologists.

MATERIALS AND METHODS

Strains

Forty-five isolates originally recovered from human and veterinary clinical specimens and belonging to the clades termed *'F.' metavorans*, FSSC 7, FSSC 9, FSSC 20 and FSSC 43 as previously defined using multilocus phylogenetic data (Zhang et al. 2006, O'Donnell et al. 2008, 2016), were retrieved from the collections of the Agricultural Research Service, Peoria, IL, USA (NRRL) and the Westerdijk Fungal Biodiversity Institute, Utrecht, The Netherlands (CBS). For morphological comparisons and phylogenetic analyses, cultures or DNA sequences from 88 additional isolates were included in the study; these isolates were obtained from the CBS, the personal collection of P.W. Crous (CPC) housed at CBS, the Fusarium Research Center housed in The Pennsylvania State University, State College, PA (FRC), the personal collection of Kerry O'Donnell (KOD), the University of Texas Health Science Center, San Antonio, TX (UTHSC), the American Type Culture Collection, Manassas, VA (ATCC), CABI Biosciences, Egham, Surrey, England (IMI) and NRRL (Table 1).

Morphology

Morphological observations and measurements of macro- and microscopic features were performed following the protocols of Aoki et al. (2003, 2005, 2013) with slight modifications as described previously (Sandoval-Denis et al. 2018). Macroscopic characteristics of fungal growth were evaluated using cornmeal agar (CMA), oatmeal agar (OA) and potato dextrose agar (PDA) (recipes in Crous et al. 2009). Colony morphology, colour, odour and presence of diffusible pigments were recorded after cultures had grown 7 d at 25 °C in darkness, under continuous fluorescent light and using a 12/12 h cool fluorescent light/dark cycle. For growth rate experiments, cultures were made on PDA agar, by transferring 5 × 5 mm agar blocks from 7-d-old cultures growing on synthetic nutrient poor agar (SNA; Nirenberg 1976). These cultures were incubated in darkness at temperatures ranging from 6–40 °C in 3 °C intervals. Growth rates were recorded after 3 and 7 d by measuring the radial colonial size in at least four directions. The micromorphological examination was made using water as mounting medium, with material taken from cultures on SNA with and without sterilised pieces of carnation leaves, incubated at room temperature (Snyder & Hansen 1947, Fisher et al. 1982, Leslie & Summerell 2006) under a 12/12 h cool fluorescent light/dark cycle. Photographs and measurements were done using a Nikon Eclipse 80i microscope with Differential Interference Contrast (DIC) optics and a Nikon AZ100 stereomicroscope, both equipped with a Nikon DS-Ri2 high definition colour digital camera, and a Nikon SMZ1000 stereomicroscope equipped with a Nikon DS-Fi1 colour digital camera. Digital images were processed using the Nikon software NIS-elements D software v. 4.50. Measurements were taken for each structure from at least 30 randomly selected elements and the mean values, SD and maximum–minimum values were calculated. Line drawings were made from microphotographs using Adobe Illustrator CS5.1 v. 15.1.0.

DNA extraction, PCR amplification and sequencing

Isolates were grown for 7–10 d on malt extract agar (MEA) plates, incubated under continuous fluorescent light at room temperature. Total genomic DNA was isolated from fresh mycelium scraped from the agar surface using the Wizard® Genomic DNA purification Kit (Promega Corporation, Madison, WI, USA) according to the manufacturer's instructions. Four gene fragments, including the internal transcribed spacer region of the rDNA (ITS), a partial fragment of the large subunit of the rDNA (LSU) (spanning the variable domains D1 to D3), two fragments of the RNA polymerase's second largest subunit (*RPB2*) and a portion of the translation elongation factor 1-alpha (*EF-1α*) were PCR amplified and sequenced according to previously published protocols (Sandoval-Denis et al. 2018) using the following primer pairs: ITS4/ITS5 for ITS (White et al. 1990), LR0R/LR5 for LSU (Vilgalys & Hester 1990, Vilgalys & Sun 1994), 5f2/7cr and 7cf/11ar for *RPB2* (Liu et al. 1999, Sung et al. 2007) and EF-1/EF-2 for *EF-1α* (O'Donnell et al. 1998). Consensus sequences were assembled from forward and reverse sequences using Seqman Pro v. 10.0.1 (DNASTAR, Madison, WI, USA). All sequences newly generated in this study were uploaded to GenBank and the European Nucleotide Archive (Table 1).

Phylogenetic analyses

Alignments of sequences of the four individual loci were made using MAFFT v. 7 (Katoh & Standley 2013) under the European Bioinformatics Institute (EMBL-EBI https://www.ebi.ac.uk) framework (Li et al. 2015), visually checked and manually corrected if needed using MEGA v. 7 (Kumar et al. 2016). The best evolutionary model for each dataset (GTR+I+G) was calculated using MrModeltest v. 2.3 (Nylander 2004). Phylogenetic inferences were made using three independent algorithms, Maximum Likelihood (ML), Maximum Parsimony (MP) and Bayesian analysis (BA), for each locus. The individual gene trees were assessed for incongruence by checking their individual

Table 1 Origin, culture and DNA sequence accession numbers of the isolates included in this study.

Species name	Lineage name[a]	Strain code[b]	Host/Sample	Country	GenBank/EMBL accession number[c]			
					EF-1α	ITS	LSU	*RPB2*
'Fusarium' brasiliense		NRRL 31757	*Glycine max*	Brazil	EF408409	EF408514	FJ919513	EU329565
'Fusarium' euwallaceae	FSSC 36	CBS 135854^{T} = NRRL 54722	*Euwallacea* sp.	Israel	JQ038007	JQ038014	JQ038014	JQ038028
	FSSC 36	NRRL 62626	*Euwallacea* sp.	USA	KC691532	KC691560	KC691560	KU171702
'Fusarium' solani f. sp. *batatas*	FSSC 23	NRRL 22400	*Ipomoea batatas*	USA	AF178343	AF178407	DQ236345	EU329509
'Fusarium' solani f. sp. *pisi*	FSSC 11	NRRL 22278	*Pisum sativum*	USA	AF178337	DQ094309	DQ236351	EU329501
	FSSC 11	NRRL 22820	*Glycine max*	USA	AF178355	DQ094310	DQ236352	EU329532
'Fusarium' solani f. sp. *xanthoxyli*	FSSC 22	NRRL 22277	*Xanthoxylum* sp.	Japan	AF178336	AF178401	AF178370	FJ240380
'Fusarium' striatum	FSSC 21	NRRL 22101	Cotton cloth	Panama	AF178333	AF178398	AF178367	EU329490
	FSSC 21	NRRL 52699	Unknown	Unknown	JF740782	JF740905	JF740905	JF741108
Geejayeesia atrofusca		NRRL 22316	*Staphylea trifolia*	USA	AF178361	AF178423	AF178392	JX171609
Geejayeesia cicatricum		CBS 125552	*Buxus sempervirens*	Slovenia	HM626644	HQ728145		HQ728153
Neocosmospora catenata	FSSC 43	NRRL 54992	Zebra shark multiple tissues	USA	KC808213	KC808255	**MG189913**	KC808354
	FSSC 43	NRRL 54993^{T}	Zebra shark multiple tissues	USA	KC808214	KC808256	**MG189914**	KC808355
Neocosmospora croci		CBS 115659	Potato	Germany	JX435156	JX435206	JX435206	JX435256
		CBS 142423^{T}	*Citrus sinensis*	Italy	LT746216	LT746264	LT746264	LT746329
		CPC 27187	*Citrus sinensis*	Italy	LT746217	LT746265	LT746265	LT746330
Neocosmospora cyanescens	FSSC 27	CBS 518.82^{T} = NRRL 37625	Human foot	The Netherlands	FJ240353	EU329684	EU329684	EU329637
Neocosmospora falciformis	FSSC 3+4	CBS 318.73 = NRRL 22660	*Trichosanthes dioica*	India	JX435158	JX435208	JX435208	JX435258
	FSSC 3+4	CBS 475.67^{T}	Human	Puerto Rico	**LT906669**	**MG18993**	**MG189915**	**LT960558**
	FSSC 3+4	NRRL 54219	Human spine	USA	HQ401721	*	*	HQ401723
Neocosmospora gamsii	FSSC 7	CBS 217.53 = NRRL 22655	Plywood	Nigeria	DQ247637	**MG189936**	**MG189916**	**LT960559**
	FSSC 7	CBS 700.86 = NRRL 22236	Unknown	Brazil	DQ247624	DQ094763	**MG189917**	**LT960560**
	FSSC 7	CBS 130181 = NRRL 43502	Human eye	USA	DQ790488	DQ790532	DQ790532	DQ790576
	FSSC 7	CBS 143207^{T} = NRRL 32323	Human bronchoalveolar lavage fluid	USA	DQ246951	DQ094420	DQ236462	EU329576
	FSSC 7	CBS 143209 = NRRL 32770	Human eye	USA	DQ247083	DQ094544	DQ236586	EU329615
	FSSC 7	CBS 143211 = NRRL 32794	Collant fluid humidifier	USA	DQ247103	DQ094563	DQ236605	EU329622
Neocosmospora haematococa		CBS 119600^{ET}	Dying tree	Sri Lanka	DQ247510	KM231797	KM231664	**LT960561**
Neocosmospora illudens		NRRL 22090	*Beilschmiedia tawa*	New Zealand	AF178326	AF178393	AF178362	JX171601
Neocosmospora keratoplastica	FSSC 2	CBS 490.63^{T}	Human	Japan	**LT906670**	*	*	**LT960562**
	FSSC 2	NRRL 43373	Contact lens	Malaysia	EF452920	EF453072	EF453072	EF469959
	FSSC 2	NRRL 43458	Human	Singapore	DQ790511	EU329686	EU329686	DQ790599
Neocosmospora lichenicola	FSSC 16	NRRL 28030	Human	Thailand	DQ246877	DQ094355	DQ236397	EF470146
	FSSC 16	NRRL 34123	Human eye	India	DQ247192	DQ094645	DQ236687	EU329635
Neocosmospora macrospora		CBS 142424^{T}	*Citrus sinensis*	Italy	LT746218	LT746266	LT746281	LT746331
		CPC 28192	*Citrus sinensis*	Italy	LT746219	LT746267	LT746282	LT746332
		CPC 28193	*Citrus sinensis*	Italy	LT746220	LT746268	LT746283	LT746333
Neocosmospora mahasenii		CBS 119594^{T}	Dead branch of live tree	Sri Lanka	DQ247513	JF433045	JF433045	**LT960563**
Neocosmospora metavorans	FSSC 6	CBS 130400 = NRRL 43489	Human cornea	USA	DQ790484	DQ790528	DQ790528	DQ790572
	FSSC 6	CBS 143194 = NRRL 22782	Human corneal ulcer	Spain	DQ246850	EU329670	EU329670	EU329528
	FSSC 6	CBS 143195 = NRRL 22792	Human eye	USA	DQ246854	EU329671	EU329671	EU329531
	FSSC 6	CBS 143198 = NRRL 28016	Human	USA	DQ246873	EU329673	EU329673	EF470140
	FSSC 6	CBS 143199 = NRRL 28017	Human	USA	DQ246874	*	FJ240359	EF470141
	FSSC 6	CBS 143200 = NRRL 28018	Human	USA	DQ246875	*	FJ240360	EF470142
	FSSC 6	CBS 143201 = NRRL 28019	Human	USA	DQ246876	*	FJ240361	EF470143
	FSSC 6	CBS 143202 = NRRL 28542 = UTHSC 98-1246	Human bone	USA	DQ246883	EU329675	EU329675	EU329543
	FSSC 6	CBS 143210 = NRRL 32785 = FRC S-1123	Human toenail cancer	USA	DQ247094	*	FJ240371	EU329618
	FSSC 6	CBS 143213 = NRRL 32849 = FRC S-1355	Human eye	USA	DQ247155	EU329682	EU329682	EU329628
	FSSC 6	CBS 143215 = NRRL 37640 = UTHSC R-3564	Human	Turkey	FJ240355	EU329685	EU329685	EU329638
	FSSC 6	CBS 143216 = NRRL 43717	Human chest	USA	FJ240356	EU329688	EU329688	EF470233
	FSSC 6	CBS 143218 = NRRL 46237	Human	USA	FJ240357	*	FJ240378	FJ240411
	FSSC 6	CBS 143219 = NRRL 46708 = FMR 8634	Human foot	Spain	*	EU329717	EU329717	EU329666
	FSSC 6	F111	Unknown	Unknown	*	*	*	*
	FSSC 6	KOD418	Unknown	Unknown	*	*	*	*
	FSSC 6	NRRL 28553	Human foot	USA	DQ246894	EU329676	EU329676	EU329548
	FSSC 6	NRRL 44892	Unknown	Unknown	GU170618	GU170638	GU170638	GU170583
	FSSC 6	NRRL 44904	Unknown	Unknown	GU170621	GU170641	GU170641	GU170586
	FSSC 6	NRRL 52746	Unknown	Unknown	JF740822	JF740921	JF740921	JF740994

Table 1 (cont.)

Species name	Lineage name[a]	Strain code[b]	Host/Sample	Country	GenBank/EMBL accession number[c]			
					EF-1α	ITS	LSU	*RPB2*
Neocosmospora petroliphila	FSSC 1	NRRL 32315 = UTHSC 00-332	Human groin ulcer	USA	DQ246943	DQ094412	DQ236454	*
	FSSC 1	NRRL 46706 = FMR 8340	Human blood	Qatar	AM412594	EU329715	EU329715	EU329664
Neocosmospora plagianthi		NRRL 22632	*Hoheria glabrata*	New Zealand	AF178354	AF178417	AF178386	JX171614
Neocosmospora pseudensiformis	FSSC 33	CBS 241.93 = NRRL 53635	Human	Suriname	JX435148	JX435198	JX435198	JX435248
	FSSC 33	CBS 125729[T]	Unknown dead tree	Sri Lanka	DQ247512	KC691584	KC691584	KC691645
	FSSC 33	NRRL 22354	Bark	French Guiana	AF178338	AF178402	DQ236358	EU329504
	FSSC 33	NRRL 46517 = FRC S-1834	Unknown	Unknown	KC691555	KC691584	KC691584	KC691645
Neocosmospora solani	FSSC 5	CBS 140079[ET] = NRRL 66304 = FRC S-2364	*Solanum tuberosum*	Slovenia	KT313611	KT313633	KT313633	KT313623
	FSSC 5	NRRL 32484 = FRC S-1242	Human	USA	DQ246982	DQ094449	DQ236491	EU329583
	FSSC 5	NRRL 43474	Human eye	USA	EF452945	EF453097	EF453097	EF469984
Neocosmospora sp.	FSSC 10	NRRL 22098	Cucurbit	USA	AF178327	DQ094301	DQ236343	EU329489
	FSSC 10	NRRL 22153 = ATCC 18099	Cucurbit	Panama	AF178346	DQ094302	DQ236344	EU329492
	FSSC 12	CBS 143196 = NRRL 25392 = ATCC 32752	American lobster	USA	DQ246861	EU329672	EU329672	EU329537
	FSSC 12	CBS 143203 = NRRL 32309 = UTHSC 00-1608	Sea turtle	USA	DQ246937	DQ094407	DQ236449	EU329571
	FSSC 12	CBS 143206 = NRRL 32317 = UTHSC 99-1886	Treefish	USA	DQ246945	DQ094414	DQ236456	EU329575
	FSSC 12	CBS 143212 = NRRL 32821 = FRC S-1230	Turtle eggs	USA	DQ247128	DQ094587	DQ236629	EU329625
	FSSC 12	CBS 143220 = NRRL 54720 = UTHSC 10-3125	Lined sea horse aquarium water	USA	JQ743207	JQ743209	JQ743209	JQ743211
	FSSC 12	CBS 143221 = NRRL 54968	Bonnet head shark	USA	**LT906671**	**MG189937**	**MG189918**	KC808332
	FSSC 12	CBS 143222 = NRRL 54970 = UTHSC 05-175	Antler crab	USA	KC808195	**MG189938**	**MG189919**	KC808334
	FSSC 12	CBS 143223 = NRRL 54971 = UTHSC 05-2774	Reptile bronchus	USA	KC808196	KC808237	**MG189920**	KC808335
	FSSC 12	CBS 143225 = NRRL 54974 = UTHSC 06-1538	Honeycomb fish	USA	KC808198	KC808239	**MG189921**	KC808337
	FSSC 12	CBS 143226 = NRRL 54979 = UTHSC 06-3660	Kemps Ridley turtle	USA	KC808202	KC808244	**MG189922**	KC808342
	FSSC 12	CBS 143227 = NRRL 54982 = UTHSC 07-1869	Kemps Ridley turtle	USA	KC808205	**MG189939**	**MG189923**	KC808345
	FSSC 12	CBS 143230 = NRRL 62549 = UTHSC 08-1422	Horseshoe crab	USA	KC808220	KC808264	**MG189924**	KC808352
	FSSC 12	NRRL 22642 = ATCC 38341	*Penaceous japonicus*	Japan	DQ246844	DQ094329	DQ236371	EU329522
	FSSC 12	NRRL 22834	Lobster	Australia	DQ247663	*	*	FJ240382
	FSSC 12	NRRL 46704 = FMR 7140	Aquarium sand	Spain	*	EU329713	EU329713	EU329662
	FSSC 12	NRRL 46705 = FMR 7414	Aquarium sand	Spain	*	EU329714	EU329714	EU329663
	FSSC 13	NRRL 22161	*Robinia pseudoacacia*	Japan	AF178330	DQ094311	DQ236353	EU329494
	FSSC 13	NRRL 22162 = ATCC 18693	*Robinia pseudoacacia*	Japan	DQ247561	EU329667	EU329667	EU329495
	FSSC 13	NRRL 22586	*Robinia pseudoacacia*	Japan	AF178353	AF178416	AF178385	EU329516
	FSSC 14	CBS 130177 = NRRL 22611	Human cornea	USA	DQ246841	DQ094326	DQ236368	EU329518
	FSSC 14	NRRL 32705 = FRC S-0390	Human skin	USA	DQ247025	DQ094488	DQ236530	EU329594
	FSSC 15	NRRL 28009	Human	USA	DQ246869	DQ094351	DQ236393	EF470136
	FSSC 15	NRRL 32792 = FRC S-1143	Human cutaneous nodules	Japan	DQ247101	DQ094561	DQ236603	EU329621
	FSSC 17	NRRL 22157 = NRRL 22479 = ATCC 18689	*Morus alba*	Japan	AF178359	DQ094306	DQ236348	EU329493
	FSSC 17	NRRL 22230 = ATCC 44934	*Morus alba*	Japan	AF178358	DQ094305	DQ236347	EU329499
	FSSC 18	NRRL 31158	Human	USA	DQ246916	DQ094389	DQ236431	EU329559
	FSSC 19	CBS 571.94 = NRRL 36510	*Camelia sinensis*	India	KC691530	KC691558	KC691558	KC691619
	FSSC 19	NRRL 20438 = IMI 296597	*Camelia sinensis*	India	AF178332	AF178397	DQ236357	JX171584
	FSSC 19	NRRL 22346	*Camelia sinensis*	India	FJ240350	EU329669	EU329669	EU329503
	FSSC 24	CBS 117481 = NRRL 22389	*Liriodendron tulipifera*	USA	AF178340	AF178404	DQ236356	EU329506
	FSSC 25	CBS 102824 = NRRL 53598	Leaf litter	Colombia	JX435147	JX435197	JX435197	JX435247
	FSSC 25	CBS 130328 = NRRL 31169	Human oral wound	USA	DQ246923	DQ094396	DQ236438	KR673999
	FSSC 26	NRRL 28541 = UTHSC 98-1305	Human synovial fluid	USA	DQ246882	EU329674	EU329674	EU329542
	FSSC 28	CBS 109028 = NRRL 32437	Human subcutaneous nodule	Switzerland	DQ246979	DQ094446	DQ236488	EU329581
	FSSC 28	NRRL 52705	Unknown	Unknown	JF740787	*	*	JF741113
	FSSC 29	KOD253	Unknown	Unknown	*	*	*	*
	FSSC 29	NRRL 28008	Human	USA	DQ246868	DQ094350	DQ236392	EF470135
	FSSC 34	NRRL 46596	Unknown	Unknown	GU170627	GU170647	GU170647	GU170592
	FSSC 34	NRRL 46703 = FMR 8281	Nematode	Spain	HM347126	EU329712	EU329712	EU329661
	FSSC 35	NRRL 46707 = FMR 8030	Human	Brazil	HM347127	EU329716	EU329716	EU329665
	FSSC 37	NRRL 25137	Diseased cocoa pods	New Guinea	JF740757	JF740899	JF740899	JF741084
	FSSC 37	NRRL 25138	Diseased cocoa pods	New Guinea	DQ247537	JF740900	JF740900	JF741085
	FSSC 38	NRRL 52782	*Hypothenemus hampei* adult	Benin	*	JF740850	JF740850	JF741176
	FSSC 38	NRRL 52783	*Hypothenemus hampei* adult	Uganda	JF740851	*	*	JF741177
	FSSC 40	F1285	Unknown	Unknown	*	*	*	*
	FSSC 45	KOD614	Unknown	Unknown	*	*	*	*

Table 1 (cont.)

Species name	Lineage name[a]	Strain code[b]	Host/Sample	Country	GenBank/EMBL accession number[c]			
					EF-1α	ITS	LSU	*RPB2*
Neocosmospora suttoniana	FSSC 20	CBS 124892	Human nail	Gabon	JX435139	JX435189	JX435189	JX435239
	FSSC 20	CBS 130178 = NRRL 22608 = UTHSC 93-1547	Human	USA	DQ246838	DQ236365	DQ094323	EU329517
	FSSC 20	CBS 143197 = NRRL 28000	Human blood	USA	DQ246865	DQ094347	DQ236389	EF470128
	FSSC 20	CBS 143204 = NRRL 32316 = UTHSC 00-264	Human corneal ulcer	USA	DQ246944	DQ094413	DQ236455	EU329574
	FSSC 20	CBS 143214^{T} = NRRL 32858	Human wound	USA	DQ247163	DQ094617	DQ236659	EU329630
	FSSC 20	CBS 143224 = NRRL 54972 = UTHSC 05-2900	Equine eye	Unknown	KC808197	**MG189940**	**MG189925**	KC808336
	FSSC 20	NRRL 28001	Human skin	USA	DQ246866	DQ094348	DQ236390	EF470129
Neocosmospora tonkinensis	FSSC 9	CBS 115.40^{T} = NRRL 53586 = IMI 113868	*Musa sapientum*	Vietnam	**LT906672**	**MG189941**	**MG189926**	**LT960564**
	FSSC 9	CBS 143038	Human cornea	The Netherlands	**LT906673**	**MG189942**	**MG189927**	**LT960565**
	FSSC 9	CBS 143208 = NRRL 32755 = FRCS-0452	Turtle head lesion	USA	DQ247073	DQ094534	DQ236576	EU329613
	FSSC 9	CBS 143217 = NRRL 43811	Human cornea	USA	EF453053	EF453204	EF453204	EF470092
	FSSC 9	FRC S-2484	Unknown	Unknown	*	*	*	*
	FSSC 9	FRC S-2540	Unknown	Unknown	*	*	*	*
	FSSC 9	NRRL 46615	Unknown	Unknown	GU250543	GU250666	GU250666	GU250728
	FSSC 9	NRRL 46676	Unknown	Unknown	GU250546	GU250669	GU250669	GU250731
Neocosmospora vasinfecta	FSSC 8	CBS 130182 = NRRL 43467	Human	USA	EF452940	EF453092	EF453092	EF469979
	FSSC 8	NRRL 34174 = UTHSC 03-1457	Human	USA	*	*	*	EU329636

[a] Following the clade nomenclature by O'Donnell et al. (2008).

[b] CBS = Westerdijk Fungal Biodiversity Institute, Utrecht, The Netherlands; CPC = Personal collection of Pedro W. Crous, held at CBS; FMR = Facultat de Medicina, Universitat Rovira i Virgili, Reus, Spain; FRC = Fusarium Research Center housed in The Pennsylvania State University, State College, PA, USA; IMI = CABI Genetic Resource Collection, Surrey, UK; KOD = personal collection of Kerry O'Donnell; NRRL = collections of the Agricultural Research Service, Peoria, IL, USA; All others = as named in K. O'Donnell's sequence database. Ex-type and ex-epitype strains are indicated with ^{T} and ^{ET}, respectively.

[c] EMBL = The European Molecular Biology Laboratory; EF-1α = partial fragment of the translation elongation factor 1-alpha; ITS = Internal transcribed spacer region of the rDNA; LSU = partial fragment of the large ribosomal subunit gene; *RPB2* = partial fragment of the DNA-directed RNA polymerase II, second largest subunit. Accession numbers of sequences generated in this study are in **bold**. Sequences marked with * were provided by Kerry O'Donnell and are not currently publicly available.

phylogenies for conflicts between clades with significant ML, MP and BA support, after which the four gene datasets were concatenated (Mason-Gamer & Kellogg 1996, Wiens 1998).

Maximum Likelihood and BA were run on the CIPRES Science Gateway portal (https://www.phylo.org/) (Miller et al. 2012) using RaxML v. 8.2.10 (Stamatakis 2014) and MrBayes v. 3.2.6 (Huelsenbeck & Ronquist 2001, Ronquist & Huelsenbeck 2003), respectively. For ML analyses the default parameters were used and BS was carried out using the rapid bootstrapping algorithm with the automatic halt option. Bayesian analyses included four parallel runs of 5 000 000 generations, with the stop rule option and a sampling frequency of 1 000 generations. The burn-in fraction was set to 0.25, after which the 50 % majority rule consensus trees and posterior probability (PP) values were calculated. The resulting trees were plotted using FigTree v. 1.4.2 (http://tree.bio.ed.ac.uk/software/figtree).

Maximum Parsimony analyses were carried out using PAUP v. 4.0b10 (Swofford 2002). Heuristic searches consisted of 1 000 random stepwise addition replicates, with tree bisection and reconstruction (TBR) branch swapping. All characters were equally weighted and gaps were treated as missing data. Zero length branches were collapsed and all multiple, equally parsimonious trees were saved. Tree length, consistency index, retention index and rescaled consistency index (TL, CI, RI and RC, respectively) were calculated. Statistical support for the branches was evaluated using a bootstrap analysis (BS) of 1 000 replicates.

RESULTS

Phylogenetic assessment of pathogenic clades in Neocosmospora

To show the current known diversity in *Neocosmospora* as well as the phylogenetic position and genealogical exclusivity of the most important lineages containing human and veterinary pathogens, an overview phylogeny was constructed based on the original alignments published by O'Donnell et al. (2008).

Individual gene phylogenies proved to be topologically consistent with each other, but showed different degrees of resolution for the most relevant pathogenic clades (data not shown, all trees available in TreeBASE). As evaluated on the basis of clade stability and ML BS values, *RPB2* was the only locus unambiguously identifying all the clinically significant clades, including '*Fusarium*' *metavorans*, FSSC 7, 9, 12, 20 and 43, as well as the important human and veterinary pathogens *N. falciformis*, '*F.*' *keratoplasticum*, '*F.*' *petroliphilum* and *N. solani*. Bootstrap values were between 93 and 100 %, except in the case of FSSC 9, where the BS was 76 %. The partitioned analysis of *EF-1α* resulted in moderate to highly supported monophyletic clades (BS = 75–100 %) for most of the pathogenic species with exception of FSSC 43. This analysis exposed considerable divergence among *EF-1α* sequences for strains within FSSC 7 and '*F.*' *keratoplasticum*; the divergent strains formed sister lineages to the respective main clades. These subclades had low statistical support. The ITS phylogeny was able to clearly distinguish five of the most important lineages, *N. falciformis*, *N. solani*, '*F.*' *petroliphilum*, FSSC 12 and FSSC 20, with BS = 76–99 %, while LSU allowed for the identification of only two pathogenic clades, FSSC 12 and FSSC 20, with BS = 71 and 92 %, respectively.

The final analysis included 3 287 characters from four loci (*EF-1α* = 675, ITS = 491, LSU = 485, *RPB2* = 1 636) of 132 strains including the outgroup taxa '*F.*' *cicatricum* = *Geejayessia cicatricum* and '*F.*' *staphyleae* = *G. atrofusca* (Schroers et al. 2011, 2016). Of the characters used, 2 297 were variable (*EF-1α* = 395, ITS = 343, LSU = 441, *RPB2* = 1 118) and 742

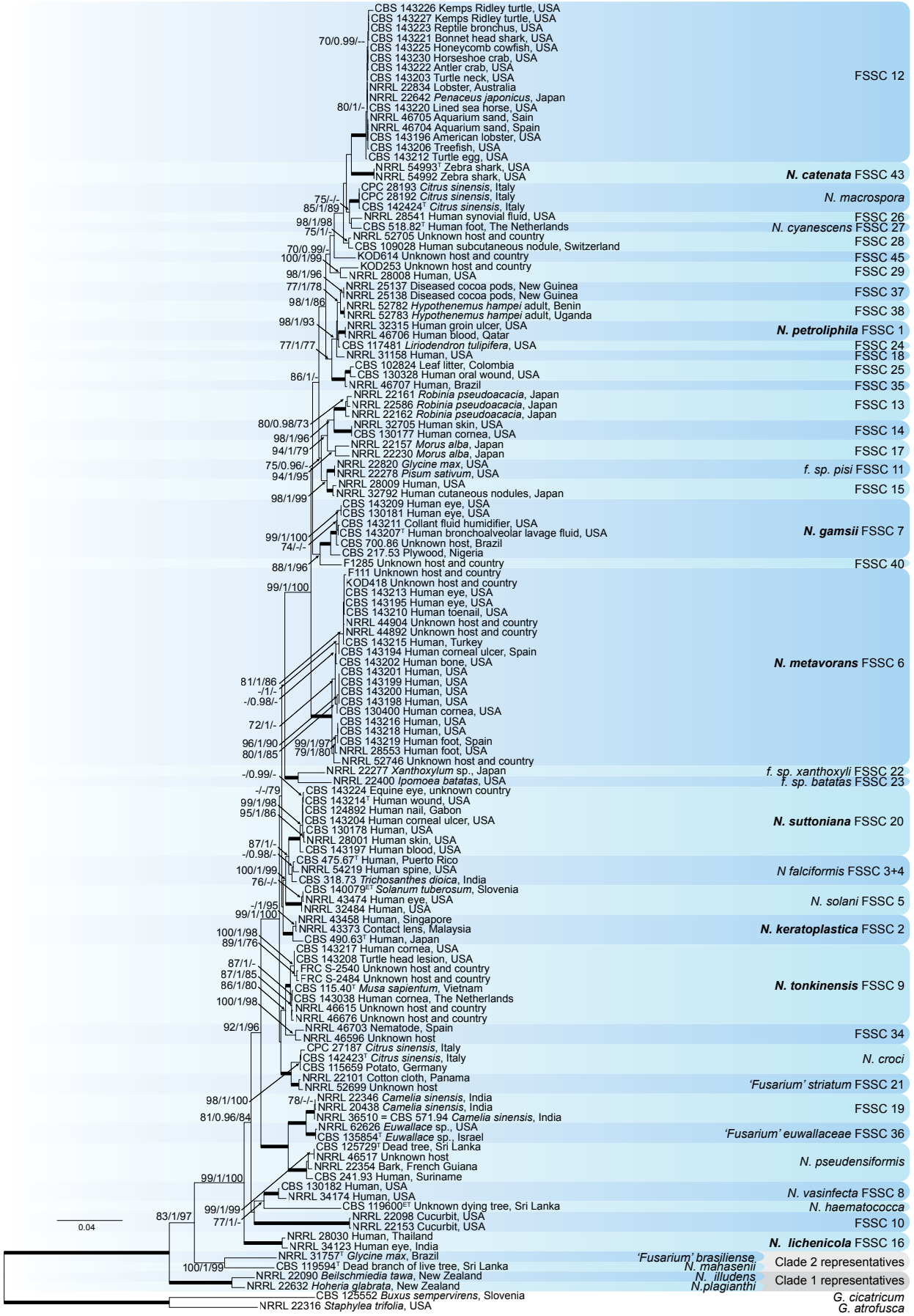

Fig. 1 Maximum likelihood (RaxML) tree obtained by phylogenetic analysis of the combined *EF-1α*, ITS, LSU and *RPB2* datasets of the genus *Neocosmospora*. Bootstrap support values from Maximum Likelihood (ML-BS), Maximum Parsimony (MP-BS) and Bayesian posterior probabilities (PP) above 70 % and 0.95, respectively, are indicated at the nodes. Nodes with full statistical support (ML-BS = 100, MP-BS = 100 and BS = 1) are indicated by **bold** branches. Names of new species and new combinations are in **bold**. *Geejayessia atrofusca* (CBS 125552) and *G. cicatricum* (NRRL 22316) were used as outgroup. CBS = Westerdijk Fungal Biodiversity Institute, Utrecht, The Netherlands; CPC = Personal collection of Pedro W. Crous, held at CBS; FRC = Fusarium Research Center housed in The Pennsylvania State University, State College, PA, USA; KOD = personal collection of Kerry O'Donnell; NRRL = collections of the Agricultural Research Service, Peoria, IL, USA; All others = as named in O'Donnell's sequence database; ET = ex-(epi-)type strain; T = ex-(holo-)type strain.

were parsimony-informative (*EF-1α* = 207, ITS = 97, LSU = 33, *RPB2* = 405). The ML search revealed a best tree with a lnL of -19162.599 (Fig. 1). The MP analysis produced 1 000 equally parsimonious trees (TL = 2 655 steps, CI = 0.489, RI = 0.830, RC = 0.406) highly congruent with that produced in ML. The BA lasted for 970 000 generations and the 50 % consensus tree and posterior probabilities were calculated from 728 trees (Fig. 1). The genus *Neocosmospora* received maximal statistical support (ML and MP BS = 100 % / 100 % and PP = 1). All human and veterinary pathogenic clades clustered within clade 3 of *Neocosmospora* sensu O'Donnell et al. (2008). All lineages containing clinically relevant unnamed phylogenetic species and currently known species resolved as monophyletic clades with strong statistical support (ML and MP BS = 100 % / 100 % and PP = 1) with exception of *N. falciformis*. This species lacked BS support in both ML and MP analyses, but had moderate BA support (PP = 0.98). The strain CBS 217.53, which showed a divergent *EF-1α* sequence, is provisionally retained here in clade FSSC 7 based on its morphological features. Clades FSSC 7, 20 and 43 are here described as the new species *N. gamsii*, *N. suttoniana* and *N. catenata*, respectively. The ex-type strain of *Cylindrocarpon tonkinense* (CBS 115.40) was found to cluster within FSSC 9, for which the new combination *Neocosmospora tonkinensis* is proposed. The recently described species '*F.' metavorans* (Al-Hatmi et al. 2018), is here recombined in *Neocosmospora* and an emended description is provided.

Taxonomy and morphology

Based on the phylogenetic evidence and morphological observations compiled here, formal descriptions for the most clinically important unnamed clades in *Neocosmospora* are provided. In keeping with the current circumscription of the genus (Lombard et al. 2015), new combinations are needed for other clinically relevant species in *Neocosmospora*.

A summary of the main morphological features (Table 2), and a schematic overview comparison (Fig. 2) were produced to facilitate the distinction of the most frequently isolated pathogens within the genus.

Neocosmospora catenata Sandoval-Denis & Crous, *sp. nov.* — MycoBank MB822898; Fig. 3

Etymology. From Latin *catena*, meaning 'chain, succession'. Referring to the abundant chains of chlamydospores.

Type. USA, Georgia, *Stegostoma fasciatum* multiple tissues (CBS H-23225 – holotype; CBS 143229 = NRRL 54993 = UTHSC 09-1009 – culture ex-type).

Sporulation abundant from conidiophores formed directly on the substrate mycelium. *Conidiophores* up to 480 µm tall, erect, emerging from the agar surface as single phialides, unbranched or more commonly 1–3-times branched laterally bearing terminal monophialides; *phialides* subulate, subcylindrical to somewhat acicular, smooth- and thin-walled, (10.5–)32.5–55(–61.5)

Table 2 Main asexual morphological features of the most clinically relevant *Neocosmospora* species.

Species name[a]	Aerial conidia	Sporodochial conidia (number of septa)	Chlamydospore diam
N. catenata	(0(–1)-septate) (4.5–)6–9(–11) × (2.5–)3.5–4.5(–6) µm	N.A.	5.5–9.5 µm, smooth-walled
N. falciformis#,†	(0–1-septate) 4.7–41.8 × 3.1–9.4 µm	(3–4-septate) Overall: 41.7–46.9 × 5.9–6.1 µm	8–15 µm, rough-walled
N. gamsii	(0(–1)-septate) (5–)6.5–9.5(–11) × 2.5–3.5(–4.5) µm	((3–)4–5(–7)-septate) (3): 35.5–42.5 × 5.5–6 µm (4): (36–)38.5–59(–63) × 5–5.5(–6) µm (5): (50.5–)55–66(–71.5) × (4.5–)5–6.5(–7) µm (6): 67–77.5 × 5.5–6.5 µm (7): 67.5–71 × 6–7 µm Overall: (35.5–)51–68(–77.5) × (4.5–)5–6(–7) µm	5.5–8(–9) µm, smooth-walled
N. keratoplastica#	(0–3-septate) 3.1–35.8 × 2.9–6.6 µm	((1–)3–5-septate) Overall: 36.8–43.4 × 5.3–5.7 µm	6.0–8.0 µm, smooth- to rough-walled
N. metavorans	(0–1(–3)-septate) (4–)11–25.5(–35) × (2–)4–6(–7) µm	((1–2–)3–5-septate) (1): 22.5–25 × 5–5.5 µm (2): 25.5–27.5 × 6–7 µm (3): (30.5–)38–46(–47.5) × (5–)5.5–6.5(–7.5) µm (4): (43–)45–48.5 × (5.5–)6–7(–7.5) µm (5): (46–)47–51.5(–53) × (5.5–)6–7.5 µm Overall: (22.5–)38.5–50(–53) × (5–)6–7(–7.5) µm	5–13.5 µm, smooth-walled
N. petroliphila#	(0(–1)-septate) 4.6–24.9 × 2.6–7.1 µm	(3–5-septate) Overall: 44–52.2 × 5.1–5.9 µm	smooth-walled
N. solani‡	(0–3(–4–5)-septate) (5.5–)13.5–43(–53) × (2–)3–7(–8) µm	((0–)3–4(–5)-septate) (3): (24–)36–44(–48) × (2–)4.5–6(–8) µm (4): (31–)42–48(–52) × (3–)4.5–6(–7.5) µm (5): (41–)45–51(–56) × (2.5–)4.5–6(–8) µm Overall: (24–)34–52.5(–56) × (2–)3–7.5(–8) µm	6.5–8.5 µm, rough-walled
N. suttoniana	(0–2(–3)-septate) (6–)7.5–21(–31) × (2.5–)3–5.5(–7.5) µm	((3–)5–6-septate) (3): 30.5–32.5 × 7–7.5 µm (4): (49–)50–53.5 × 6–6.5 µm (5): (30.5–)52–71(–77.5) × (6–)7–8 µm (6): (75–)77–84.5(–86.5) × (6.5–)7–8 µm Overall: (30.5–)50–75(–86.5) × (6–)7–7.5(–8) µm	(4.8–)6–8.5(–9.5) µm, verruculose
N. tonkinensis	(0–3(–4)-septate) (6–)11–24(–37) × (3.5–)4–6(–7) µm	((1–)3–4(–5)-septate) (1): 47–51 × 6–7.5 µm (3): (28–)32.5–42.5(–45.5) × (5.5–)6–7.5 µm (4): (40.5–)43–48(–49) × 6–7.5 µm (5): (40–)41.5–52 × 6.9–7.3 µm Overall: (27.5–)37–48(–50.5) × (5.5–)6–7(–7.5) µm	6.5–10(–12) µm, smooth-walled

[1] Conidial measurements from: # Short et al. (2013), † Chehri et al. (2015), ‡ Schroers et al. (2016).

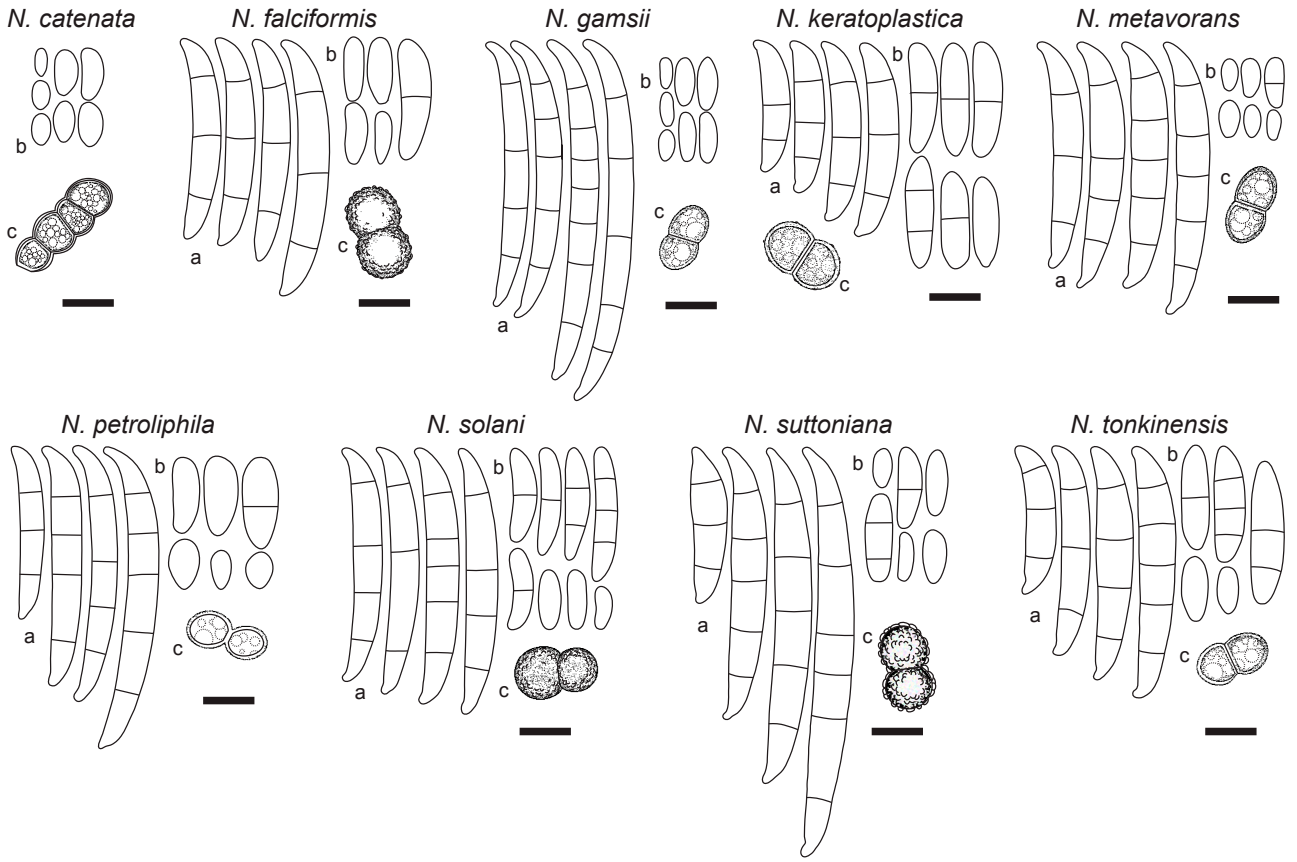

Fig. 2 Line drawings comparing the main conidial and chlamydospore features of the most clinically relevant species of *Neocosmospora*. a. Sporodochial conidia; b. aerial conidia; c. chlamydospores. — Scale bars = 10 µm.

× (1.5–)2.5–3.5(–4) µm, with distinct periclinal thickening and an apical flared collarette; *conidia* hyaline, obovate, ellipsoidal to reniform, commonly bent dorsoventrally, smooth- and thin-walled, 0(–1)-septate, (4.5–)6–9(–11) × (2.5–)3.5–4.5(–6) µm, grouped on small false heads on the tip of monophialides. *Chlamydospores* abundant, subhyaline to pale brown, spherical to subspherical, 5.5–9.5 µm diam, solitary, in pairs, chains or clusters, terminal or intercalary, smooth- and thick-walled. *Sporodochia* and multiseptate conidia not seen.

Culture characteristics — Colonies on PDA growing in the dark with an average radial growth rate of 2.5–5 and 3.5–5.9 mm/d at 21 and 24 °C, respectively, reaching 74–82 mm diam in 7 d at 24 °C and occupying an entire 9 cm Petri dish in 7 d at 27 °C. Colony surface buff to rosy buff, flat, felty to velvety, radiate, with abundant aerial mycelium; colony margins irregular with abundant submerged mycelium. Reverse straw to buff coloured. Straw to pale sulphur yellow diffusible pigment produced between 21–27 °C, becoming ochreous to umber at 30–33 °C. Colonies on OA incubated at 24 °C in the dark reaching 80–90 mm diam in 7 d. Colony buff to honey, flat, membranous, becoming velvety with the production of short aerial mycelium; margins regular. Reverse buff to honey, without diffusible pigments. A hazel to isabelline pigment can be produced in incubation at 36 °C. On CMA incubated at 24 °C in the dark, cultures occupy an entire 9 mm Petri dish in 7 d. Colony colour sulphur yellow to straw, flat with abundant floccose aerial mycelium. Reverse sulphur yellow to straw without diffusible pigments.

Cardinal temperatures for growth — Minimum 12 °C, maximum 36 °C, optimal 24–27 °C.

Additional material examined. USA, Georgia, *Stegostoma fasciatum* multiple tissues (NRRL 54992 = CBS 143228 = UTHSC 09-1008).

Notes — *Neocosmospora catenata*, known from the zebra shark (*Stegostoma fasciatum*), is well-defined phylogenetically as a fully-supported sister clade to FSSC 12, which is also known mostly from infections of marine animals. No single morphological feature exists allowing a quick phenotypic distinction of FSSC 12 from *N. catenata*, notwithstanding the tendency of the latter species to produce large, pigmented, catenate to clustered chlamydospores. The two strains studied here consistently failed to produce the characteristic falcate, multiseptate sporodochial conidia typical of the genus. Sporulation was abundant, but strictly microconidial. It is not clear if this phenomenon reflects strain degeneration or if it is a distinctive peculiarity of this clade. The two strains of *N. catenata* included in this study are, to our knowledge, the only material currently available in fungal collections. Additional isolates are needed to help in evaluating this potentially important differential morphological character.

Neocosmospora gamsii Sandoval-Denis & Crous, *sp. nov.* — MycoBank MB822899; Fig. 4, 5

Etymology. In honour and memory of Walter Gams, eminent mycologist and *Fusarium* researcher.

Type. USA, Pennsylvania, from human bronchoalveolar lavage fluid, *D.A. Sutton* (CBS H-23226 – holotype; CBS 143207 = NRRL 32323 = UTHSC 99-250 – culture ex-type).

Sporulation abundant from sporodochia and from conidiophores formed directly on the substrate mycelium. *Conidiophores* in the aerial mycelium up to 410 µm tall, irregularly or sympodially branched at various levels, bearing terminal monophialides; *phialides* subulate, subcylindrical or acicular, smooth- and thin-walled, (37.5–)46.5–64(–78) × (2–)2.5–4 µm, with inconspicuous periclinal thickening; collarettes small and barely visible; *conidia* formed on aerial conidiophores hyaline, ellipsoidal to clavate, sometimes slightly and inequilaterally bent dorsoventrally, smooth- and thin-walled, 0(–1)-septate,

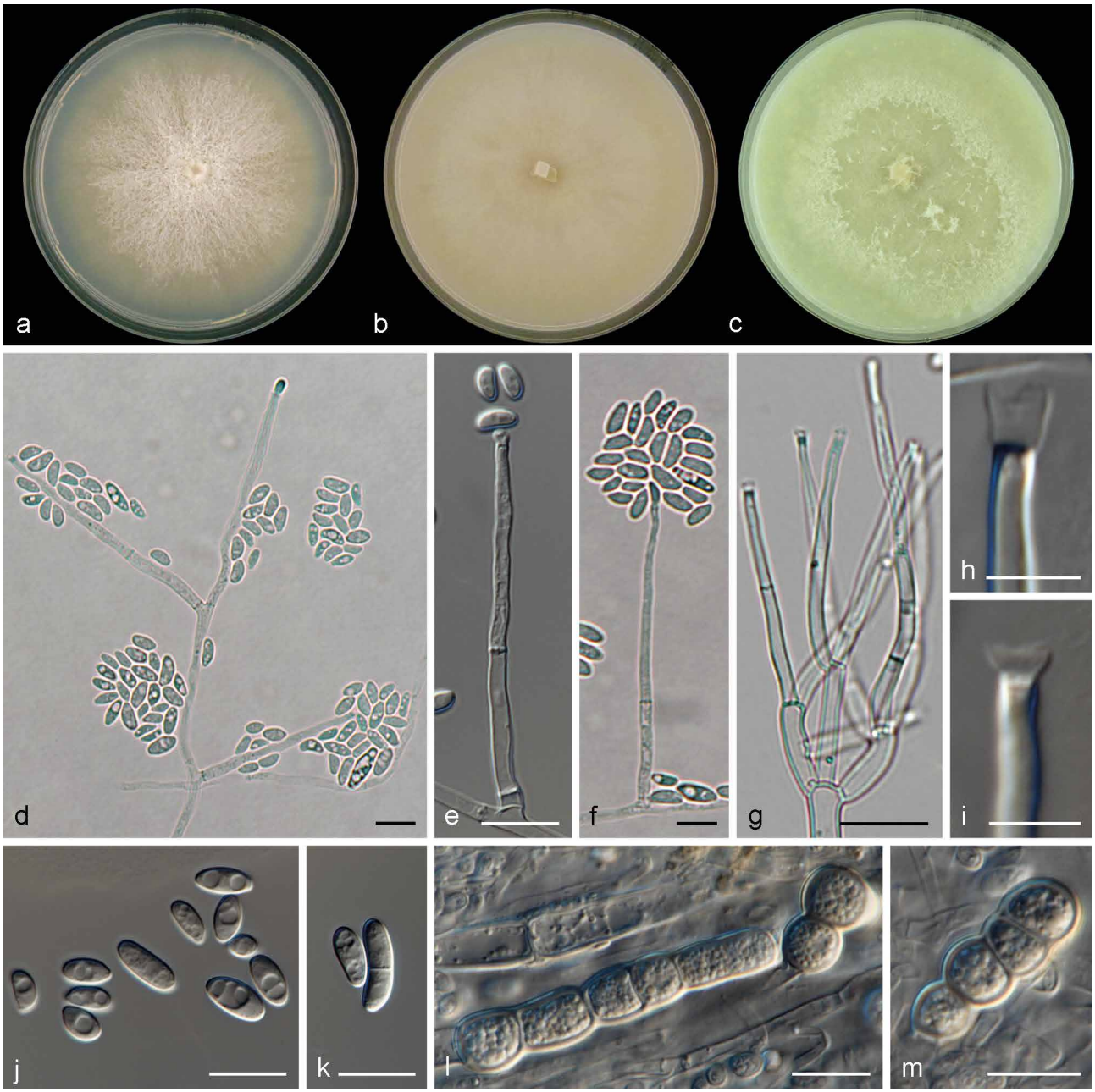

Fig. 3 *Neocosmospora catenata*. a. Colony on PDA; b. colony on OA; c. colony on CMA; d–g. conidiophores and phialides; h–i. tip of phialides showing apical collarettes; j–k. conidia; l–m. chlamydospores. — Scale bars: h–i = 5 µm; all others = 10 µm.

(5–)6.5–9.5(–11) × 2.5–3.5(–4.5) µm, single or forming small false heads. *Sporodochia* at first cream coloured turning green to yellow-blue-green, formed abundantly on the surface of carnation leaves, rapidly confluent. *Conidiophores* in sporodochia, 23–47.5 µm tall, densely packed, irregularly or verticillately branched, terminal branches bearing 1(–2) monophialides; sporodochial phialides subulate to subcylindrical or doliiform, often slightly constricted or bent in the middle portion, 12–18.5(–24) × (2.5–)3–3.5(–4) µm, smooth- and thin-walled, often showing periclinal thickening and an evident flared collarette. Sporodochial *conidia* wedge-shaped, medium to robust, with an almost straight to slightly curved ventral line and a gentle, continuous dorsal curvature, tapering and becoming more pronouncedly curved towards the basal and apical levels, apical cell more or less equally sized than the adjacent cell, distinctly hooked with rounded ends and a notched to foot-like basal cell, (3–)4–5(–7)-septate, hyaline, thin- and smooth-walled. Three-septate conidia: 35.5–42.5 × 5.5–6 µm; 4-septate conidia: (36–)38.5–59(–63) × 5–5.5(–6) µm; 5-septate conidia: (50.5–)55–66(–71.5) × (4.5–)5–6.5(–7) µm; 6-septate conidia: 67–77.5 × 5.5–6.5 µm; 7-septate conidia: 67.5–71 × 6–7 µm; overall (35.5–)51–68(–77.5) × (4.5–)5–6(–7) µm. *Chlamydospores* abundant, spherical to subspherical, 5.5–8(–9) µm diam, solitary or in pairs, terminal and intercalary, smooth- and thick-walled. *Perithecia* orange to dark brown-red, globose to pyriform, superficial, solitary or gregarious, coarsely warted, glabrous, 186–194 × 138–156 µm; warts 5–20 µm diam, 3.5–16 µm tall. *Peridial wall* composed of thick-walled cells of *textura angularis*, (7.5–)11.5–18(–20.5) µm diam. *Asci* clavate, unitunicate, with a broad and somewhat flattened and simple apex, (70–)72–87.5(–97.5) × (6.5–)7.5–9(–10) µm, ascospores obliquely uniseriate or irregularly biseriate at the apex of the asci. *Ascospores* obovoid to subfusiform, 1-septate, (9.5–)10.5–11.5(–12.5) × (4.5–)5.0–6.5(–7.5) µm, pale yellow-brown to golden yellow, thick-walled, longitudinally finely striated, often slightly constricted at the septum.

Culture characteristics — Colonies on PDA growing in the dark with an average radial growth rate of 2.5–4.6 and 3.3–5.7 mm/d at 21 and 24 °C, respectively, reaching 76–80 mm diam in 7 d at 24 °C. Colony surface pale luteous to rosy buff, flat,

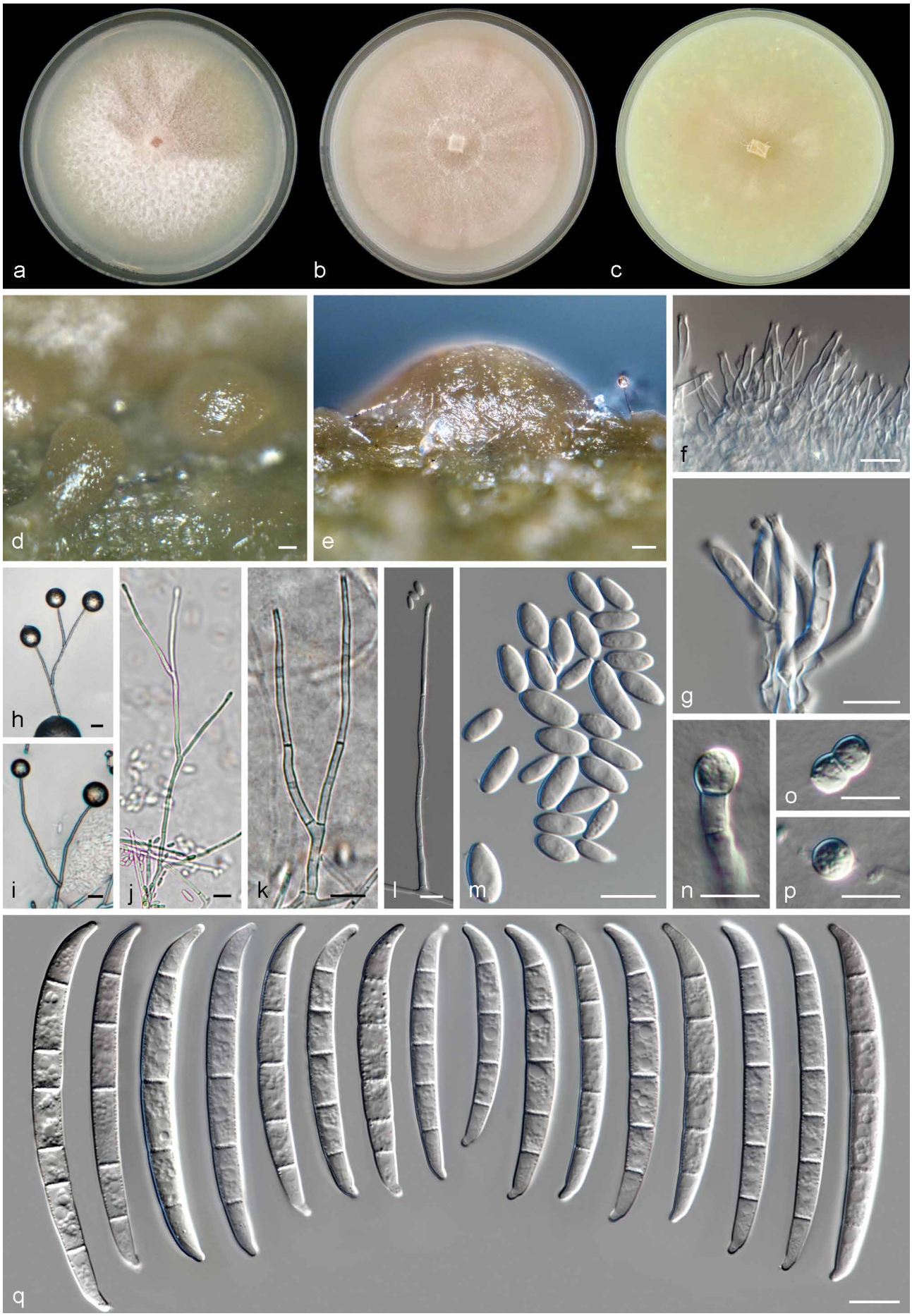

Fig. 4 *Neocosmospora gamsii*, asexual morph. a. Colony on PDA; b. colony on OA; c. colony on CMA; d–e. sporodochia formed on the surface of carnation leaves; f–g. sporodochial conidiophores and phialides; h–l. aerial conidiophores and phialides; m. aerial conidia; n–p. chlamydospores; q. sporodochial macroconidia. — Scale bars: d–e = 20 µm; all others = 10 µm.

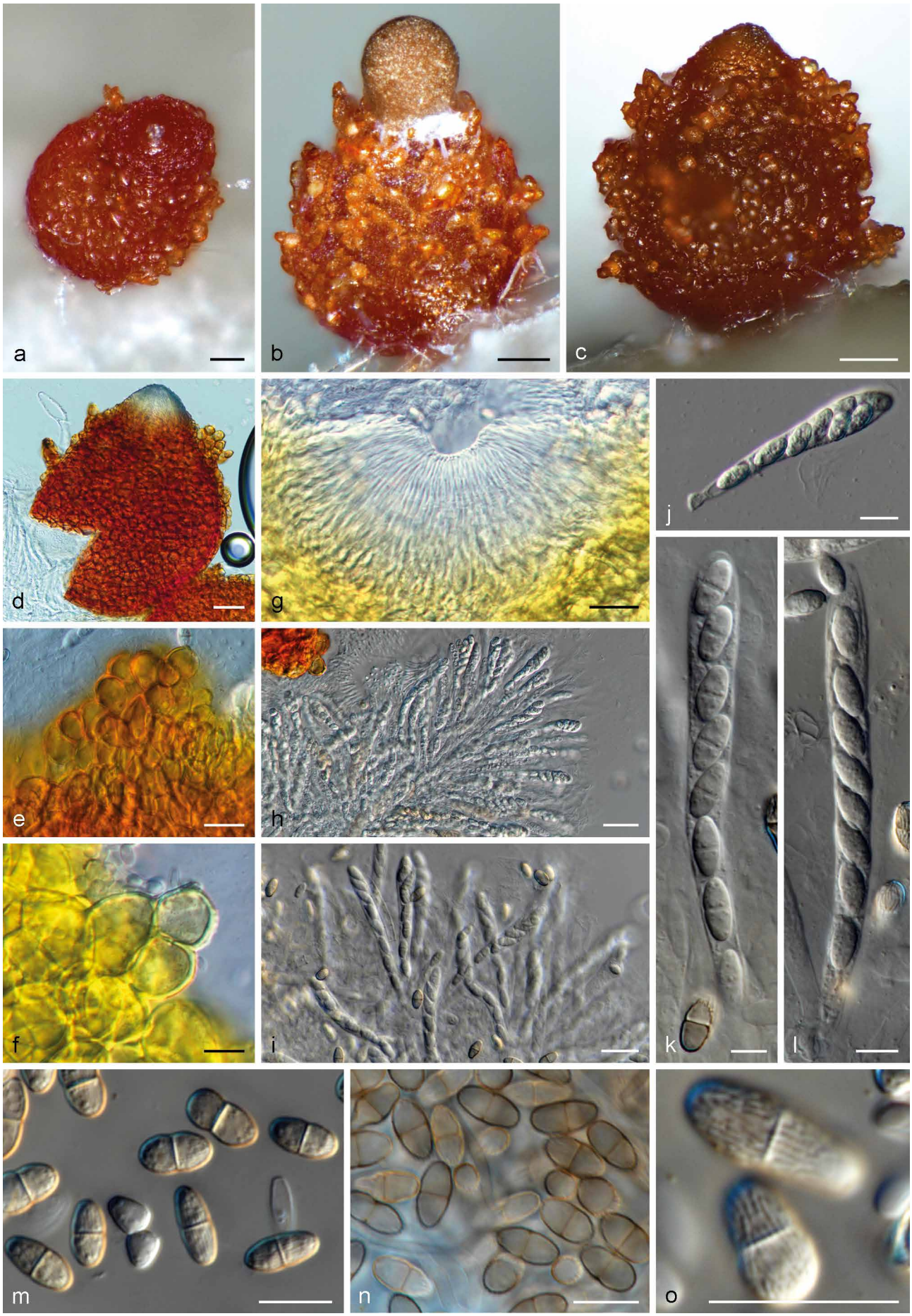

Fig. 5 *Neocosmospora gamsii*, sexual morph. a–c. Perithecia; d. perithecium showing a deep-red reaction on 3 % KOH; e. close view of perithecial warts (mounted on water); f. close view of perithecial warts showing a yellow reaction on lactic acid; g. ostiole and periphyses; h–l. asci and ascospores; m–n. ascospores; o. surface view of ascospores. — Scale bars: a–e, g–i = 20 µm; all others = 10 µm.

felty with velvety radial patches and abundant floccose white aerial mycelium; colony margins regular. Reverse pale luteous to orange or light scarlet toward the centre of the colony. Yellow to orange-yellow diffusible pigments can be formed at temperatures from 15 to 36 °C, becoming more intense as temperatures exceed 27 °C. Colonies on OA incubated at 24 °C in the dark reaching a maximum of 70–72 mm diam in 7 d. Colony surface pale rosy buff to pale rosy vinaceous, flat and radially folded, moist, bright and membranous, becoming felty to velvety or cottony with the production of abundant, short aerial mycelium often arranged in concentric rings, and becoming compact and restricted at 30–37 °C; margins regular. Reverse rosy vinaceous without diffusible pigments. On CMA incubated at 24 °C in the dark reaching a maximum of 35–40 mm diam in 7 d. Colony colour straw to pale buff with ochreous patches; colony surface flat with abundant submerged mycelium, and with rays of scant aerial mycelium. Reverse, straw to sulphur yellow without diffusible pigments.

Cardinal temperatures for growth — Minimum 9 °C, maximum 36 °C, optimal 24–30 °C.

Additional material examined. Brazil, substrate, date and collector unknown (CBS 700.86 = NRRL 22236). – Nigeria, from plywood, Feb. 1953, *M.B. Schol-Schwarz* (CBS 217.53 = NRRL 22655). – USA, Tennessee, from human eye, *M. Brandt* (CBS 130181 = NRRL 43502); Tennessee, from human eye (CBS 143209 = NRRL 32770 = FRC S-0524); New York, from humidifier coolant (CBS 143211 = NRRL 32794 = FRC S-1152).

Notes — This species was previously assigned to clade FSSC 7 in *Neocosmospora*. Morphologically *N. gamsii* resembles *Fusarium eumartii*, a known pathogen of potatoes (*Solanum tuberosum*) and tomatoes (*Lycopersicon esculentum*), for which also pathogenicity against pepper (*Capsicum anuum*) and eggplant (*Solanum melongena*) has also been demonstrated (Romberg & Davis 2006). *Fusarium eumartii*, however, has not been fully characterised phylogenetically and lacks authentic living strains for comparison. Two strains previously identified as *F. eumartii*, CBS 217.53 and CBS 700.86, were found to cluster within FSSC 7. The current concept of *F. eumartii*, however, based on morphology and host ranges, is polyphyletic, with isolates distributed among at least six monophyletic clades within *Neocosmospora* (unpubl. data). *Neocosmospora gamsii* can nonetheless be distinguished morphologically from the concept of *F. eumartii*, since it produces comparatively thin and short sporodochial conidia, which are also less frequently septate than conidia of *F. eumartii* and have a more pronounced apical curvature.

Among the clinically relevant species, *N. gamsii* stands out in its long, slender and highly septate (up to 7 septa) sporodochial conidia, comparable to those of *N. suttoniana*. The latter species, however, produces less frequently septate (up to 6 septa) sporodochial conidia with thick-walls and with a less pronounced overall curvature. It also produces rough-walled chlamydospores distinct from the smooth-walled chlamydospores seen in *N. gamsii*.

So far, this species is known mainly from human clinical specimens, causing mostly eye infections but also recovered from blood samples (Scheel et al. 2013). It was reported as one of many '*Fusarium*' genotypes recovered from patients affected by a keratitis outbreak in the US (Chang et al. 2006).

Neocosmospora keratoplastica (Geiser et al.) Sandoval-Denis & Crous, *comb. nov.* — MycoBank MB822900

Basionym. *Fusarium keratoplasticum* Geiser et al., Fungal Genet. Biol. 53: 68. 2013.

Synonyms. *Cephalosporium keratoplasticum* T. Morik, Mycopathologia 2. 66. 1939, *nom. nud.* (*fide* Short et al. 2013).

Hyalopus keratoplasticum (T. Morik) M.A.J. Barbosa, Notarisia 19. 1941, *nom. inval.* (*fide* Short et al. 2013).

Fusarium solani (Mart.) Sacc. f. *keratitis* Y.N. Ming & T.F. Yu, Acta Microbiol. Sin. 12: 184. 1966.

Cylindrocarpon vaginae C. Booth, Y.M. Clayton & Usherw., Proc. Indian Acad. Sci. Pl. Sci. 94: 436. 1985.

Type. USA, Virginia, Winchester, from indoor plumbing, June 2009 (FRC S-2477 – holotype, metabolically inactive culture deposited at the Fusarium Research Center, ex-type strain: CBS 490.63 = NRRL 22661).

Description and illustrations — Short et al. (2013).

Notes — This cosmopolitan species is known almost exclusively from infected animals and from biofilms occurring in plumbing systems, including hospital water supplies (Short et al. 2013, 2014), but is also occasionally found in plant material and soil (Chehri et al. 2015, Shaffer et al. 2017). It is regarded as one of the most prevalent fusaria isolated from human disease worldwide, causing mostly corneal infections, but also isolated from blood, nails and skin (O'Donnell et al. 2008, Short et al. 2013). It is also a common species in animal infections, and has been reported from many different species, including mostly aquatic or aquatic-adapted animals such as the black spotted stingray (*Taeniura melanopsila*) (Fernando et al. 2015), grey seal (*Halichoerus grypus*) (O'Donnell et al. 2016), hammer-head sharks (Fernando et al. 2015), iguanas (O'Donnell et al. 2008, 2016), lung fish (O'Donnell et al. 2016) and shrimps including *Penaeus japonicus* and the California brown shrimp (O'Donnell et al. 2008, 2016). It causes extensive egg mortality in the green sea turtle, *Chelonia mydas* (Sarmiento-Ramírez et al. 2017), and, together with *N. falciformis*, represents a significant risk for the endangered hawksbill sea turtle, *Eretmochelys imbricata* (Sarmiento-Ramírez et al. 2014). Terrestrial animals such as equines and *Drymarchon corais*, the indigo snake, may also be infected (O'Donnell et al. 2016).

Reported as having highly variable conidial morphology in culture (Short et al. 2013, 2014), *N. keratoplastica* frequently produces short, (1–2–)3–5-septate, arcuate sporodochial conidia somewhat reminiscent in shape of those seen in FSSC 12 (Short et al. 2013). However, the latter species produces 1–3-septate and much shorter and thinner sporodochial conidia (overall: (19–)24.5–35(–41) × 5–6(–6.5) vs 13.2–60.1 × 2.8–8.2 in *N. keratoplastica*).

Interestingly, genetic analyses have demonstrated some significant degree of genetic transfer between *N. keratoplastica* and *N. tonkinensis*, as shown by perfect sequence matches between the nuclear rDNA regions in some isolates (Short et al. 2014).

Neocosmospora lichenicola (C. Massal) Sandoval-Denis & Crous, *comb. nov.* — MycoBank MB822901

Basionym. *Fusarium lichenicola* C. Massal., Ann. Mycol. 1: 223. 1903.

Synonyms. *Bactridium lichenicolum* (C. Massal.) Wollenw., Fusaria autographica delineata 1: no. 456. 1916.

Monacrosporium tedeschii A. Agostini, Atti Ist. Bot. Lab. Crittog. Univ. Pavia. 4: 195. 1933.

Euricoa dominguiesii Bat. & H. Maia, Anais Soc. Biol. Pernambuco 13: 152. 1955.

Hyaloflorea ramosa Bat. & H. Maia, Anais Soc. Biol. Pernambuco 13: 155. 1955.

Mastigosporium heterosporum R.H. Petersen, Mycologia 51: 729. 1959.

Cylindrocarpon lichenicola (C. Massal.) D. Hawksw., Bull. Brit. Mus. (Nat. Hist.), Bot. 6: 273. 1979.

Neocosmospora ramosa (Bat. & H. Maia) L. Lombard & Crous, Stud. Mycol. 80: 227. 2015.

non *Fusarium lichenicola* (Speg.) Sacc. & Trotter, Syll. Fung. 22: 1486. 1913. *nom. Illegit.* (*fide* Hawksworth 1979).

Selenosporium lichenicola Speg., Anales Mus. Nac. Buenos Aires. 20: 459. 1910.

Type. Italy, *Verona*, Tregnago, on *Candelaria concolor*, Nov. 1902, *C. Massalongo* (holotype PAD not seen, culture ex-type not known).

Description and illustrations — Wollenweber (1916), Petersen (1959), Hawksworth (1979), Summerbell & Schroers (2002).

Notes — This species is an infrequent agent of human disease, known from localised and invasive infections such as keratitis (Champa et al. 2013), onychomycosis (Guevara-Suarez et al. 2016), mycetoma (Chazan et al. 2004), intertrigo in warm climates, disseminated infection (Rodriguez-Villalobos et al. 2003) and peritonitis (Liu 2011). In addition, it is acknowledged as a phytopathogenic agent infecting *Camellia sinensis* (Shaw 1984), and causing corm rot of *Colocasia esculenta* (Usharani & Ramarao 1981) and fruit rot of pomelo (*Citrus maxima*) (Amby et al. 2015, Farr & Rossman 2017).

Morphologically, it is clearly recognisable in comparison with all other members of the genus in producing ellipsoidal, 0–3-septate aerial conidia that possess a short, truncate base, and that are not curved or pointed like the typical conidia of *Neocosmospora* species. Sporodochia are not produced. These distinctive features led to the species being transferred in the past to the genus *Cylindrocarpon* (Hawksworth 1979). Molecular evidence showed, however, it belongs in *Neocosmospora* (Summerbell & Schroers 2002).

Neocosmospora metavorans (Al-Hatmi et al.) Sandoval-Denis & Crous, *comb. nov.* — MycoBank MB823687; Fig. 6

Basionym. *Fusarium metavorans* Al-Hatmi et al., Med. Mycol. 56: S147. 2018.

Type. Greece, Athens, from human pleural effusion, 2013, *M. Drogari* (CBS 135789 – holotype of *Fusarium metavorans*, maintained as metabolically inactive culture; CBS 135789 – culture ex-type).

Original description and illustrations — Al-Hatmi et al. (2018).

Emended description — *Sporulation* abundant from sporodochia and from conidiophores formed directly on the substrate and aerial mycelium. *Conidiophores* in the aerial mycelium up to 285 µm tall, unbranched, sympodial or irregularly branched up to three times at various levels, bearing terminal and single monophialides; *phialides* subcylindrical, smooth- and thin-walled, (9–)14–45(–62) × 4–7(–8) µm, with inconspicuous periclinal thickening and somewhat flared collarettes; *conidia* formed on aerial conidiophores hyaline, ellipsoidal, smooth- and thin-walled, 0–2(–3)-septate, (4–)11–25.5(–35) × (2–)4–6(–7) µm, single or forming small false heads. *Sporodochia* at first white, turning ochreous when mature, formed abundantly on the surface of carnation leaves and rarely on the agar surface, later clustering into dry pionnotes. *Conidiophores* in sporodochia 25–50 µm tall, verticillately branched, bearing 1–6 monophialides in terminal verticils; sporodochial phialides subulate to subcylindrical, (11–)13.5–19(–22) × 3–4.5 µm, smooth- and thin-walled, with inconspicuous periclinal thickening and a short, evident, flared collarette. Sporodochial *conidia* medium to robust, with an almost straight, rarely bent ventral line and a continuous dorsal curvature, wider above the middle portion and tapering toward the basal cell; apical cell equally sized or smaller than the adjacent cell, blunt to slightly hooked with rounded tip; basal cell discretely notched, (1–2–)3–5-septate, hyaline, thin- and smooth-walled. One-septate conidia: 22.5–25 × 5–5.5 µm; 2-septate conidia: 22.5–27.5 × 6–7 µm; 3-septate conidia: (30.5–)38–46(–47.5) × (5–)5.5–6.5(–7.5) µm; 4-septate conidia: (43–)45–48.5 × (5.5–)6–7(–7.5) µm; 5-septate conidia: (46–)47–51.5(–53) × (5.5–)6–7.5 µm; overall: (22.5–)38.5–50(–53) × (5–)6–7(–7.5) µm. *Chlamydospores* abundant, spherical to subspherical 5–13.5 µm diam, solitary or in pairs, terminal and intercalary, smooth- and thick-walled.

Culture characteristics — Colonies on PDA growing at 24 °C in the dark with an average radial growth rate of 6.3–7.1 mm/d, reaching 44–50 mm diam in 7 d. Colony surface at first white to pale straw coloured, gradually turning pale brick to pale coral, flat, felty to cottony with abundant and short aerial mycelium often arranged in concentric rings; colony margins regular. Reverse white to pale yellow or rust coloured. Colonies on OA and CMA incubated at 24 °C in the dark reaching a maximum of 60–71 and 43–50 mm diam in 7 d, respectively. Colony surface white, pale straw to pale luteous or rust coloured, flat, radiated or radially folded, velvety to cottony with abundant white aerial mycelium; colony margins regular. Reverse at first white, then producing luteous or rust coloured pigments.

Cardinal temperatures for growth — Minimum 9 °C, maximum 36 °C, optimal 24–30 °C.

Additional material examined. Spain, from human corneal ulcer, 15 Mar. 1978 (CBS 143194 = NRRL 22782 = IMI 226114); from human foot, 14 July 2004, *F. Ballester* (CBS 143219 = NRRL 46708 = FMR 8634). – Turkey, from human (CBS 143215 = NRRL 37640 = UTHSC R-3564). – USA, Maryland, from human cornea, *M. Brandt* (CBS 130400 = NRRL 43489); San Francisco, from human eye, 14 Dec. 1970 (CBS 143195 = NRRL 22792 = IMI 153617); from human (CBS 143198 = NRRL 28016); from human (CBS 143199 = NRRL 28017); from human (CBS 143200 = NRRL 28018); from human (CBS 143201 = NRRL 28019); New England, from human bone, *A. Fothergill* (CBS 143202 = NRRL 28542 = UTHSC 98-1246); Maryland, from human toenail cancer (CBS 143210 = NRRL 32785 = FRC S-1123); Texas, from human eye (CBS 143213 = NRRL 32849 = FRC S-1355); Michigan, from human chest subcutaneous tissue, 2003, *M. Brandt* (CBS 143216 = NRRL 43717); Illinois, from human, *P. Kammeyer* (CBS 143218 = NRRL 46237).

Notes — One of the most prevalent clades isolated from human clinical specimens, *N. metavorans* is known to cause superficial and deep-seated or disseminated infections (O'Donnell et al. 2008). This species has been also recovered from insects (*Ceresa bubalus*, O'Donnell et al. 2012) and from plant material (Chen & Kirschner 2017, Al-Hatmi et al. 2018). It is also one of the few species in *Neocosmospora* for which a complete genome sequence is available (Coleman 2016, Herr et al. 2016).

This species shows a considerable similitude with *N. solani* and *N. suttoniana* in overall culture characteristics and the shape of the sporodochial conidia. However, sporodochial conidia in *N. metavorans* are slightly wider with conspicuously pedicellate basal cells. By contrast, foot cells are less evident in *N. solani*. *Neocosmospora suttoniana* can be differentiated by having much longer and septate sporodochial conidia (up 86.5 µm long and 6-septate) as well as by its verruculose chlamydospores (vs up to 53 µm long and 5-septate sporodochial conidia and smooth-walled chlamydospores in *N. metavorans*). The protologue of *N. metavorans* also points to a morphological similitude with *N. solani* s.str. The former species, however, is described as being distinct in the lack of sporodochial conidia and in having conidia in long chains. The ex-type strain of *N. metavorans* may not produce sporodochial conidia, but all the clinical isolates studied here were able to produce sporodochia and multiseptate conidia under standard culture conditions, while conidial chains, which are not an expected characteristic in this genus, were not observed. A re-examination of the ex-type culture is necessary to further evaluate its description. Moreover, we observed a much wider micromorphological variation among our isolates than was noted by Al-Hatmi et al. (2018), and hence, an emended morphological description and illustrations are provided.

Neocosmospora petroliphila (Q.T. Chen & X.H. Fu) Sandoval-Denis & Crous, *comb. nov.* — MycoBank MB822902

Basionym. *Fusarium solani* (Mart.) Sacc. var. *petroliphilum* Q.T. Chen & X.H. Fu, Acta Mycol. Sin., Suppl. 1: 330. 1987.

Synonyms. *Fusarium solani* (Mart.) Sacc. f. sp. *cucurbitae* W.C. Snyder & H.N. Hansen, Amer. J. Bot. 28: 740. 1941. Race 2.

Fusarium petroliphilum (Q.T. Chen & X.H. Fu) Geiser et al., Fungal Genet. Biol. 53: 69. 2013.

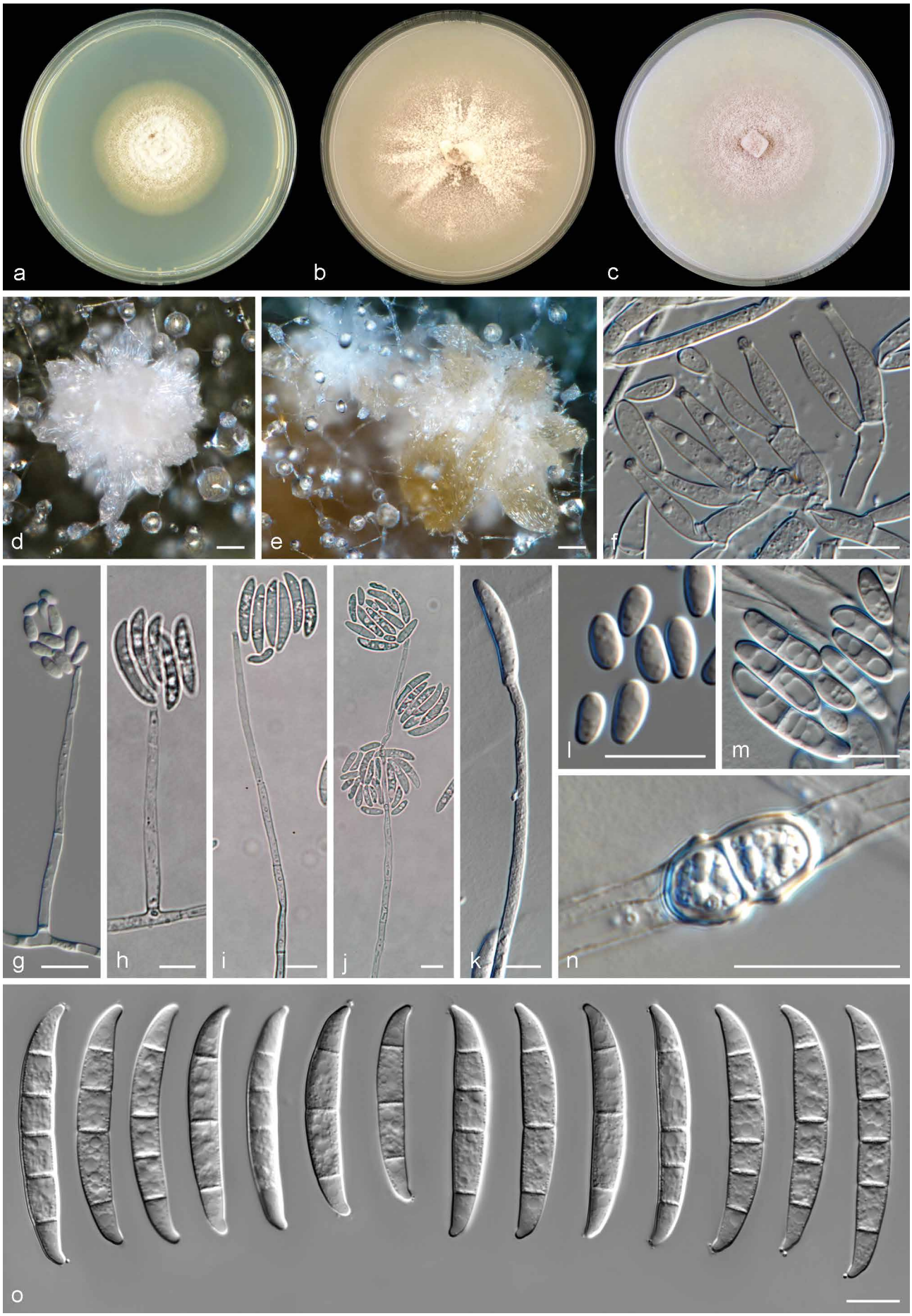

Fig. 6 *Neocosmospora metavorans*. a. Colony in PDA; b. colony in OA; c. colony in CMA; d–e. sporodochia formed on the surface of carnation leaves; f. sporodochial conidiophore and phialides; g–k. aerial conidiophores and conidia; l–m. aerial conidia; n. chlamydospores; o. sporodochial conidia. — Scale bars: a–b = 20 µm; all others = 10 µm.

Type. China, from deteriorated petroleum (NF 4475, holotype of *F. solani* var. *petroliphilum*, metabolically inactive culture deposited at the Chinese Academy of Sciences Institute of Microbiology, Beijing, not seen; ex-type strain: NF4475 = NRRL 22268 = FRC S-2176).

Description and illustrations — Short et al. (2013).

Notes — *Neocosmospora petroliphila* and *N. keratoplastica* are the two most prevalent fusaria species in human clinical samples and are regarded as the most important agents of keratitis (Zhang et al. 2006, O'Donnell et al. 2007). Other known isolation sites of *N. petroliphila* from humans include blood (O'Donnell et al. 2008, Ersal et al. 2015), nails (Zhang et al. 2006, Guevara-Suarez et al. 2016), nasal mucosa and skin (Zhang et al. 2006, Ersal et al. 2015). Abiotic environments yielding this fungus include contact lens solution and ceiling plaster (O'Donnell et al. 2008). *Neocosmospora petroliphila* also occurs as the predominant species producing biofilms in plumbing systems together with *N. keratoplastica* (Mehl & Epstein 2008, Short et al. 2013). The species can infect animals, mostly those with aquatic habitats, such as cetaceans and fish (O'Donnell et al. 2016). It is a recognised agent of fruit rot on cucurbits (Toussoun & Snyder 1961, O'Donnell 2000).

Neocosmospora petroliphila was previously regarded as roughly distinguishable by forming 3–5-septate, falcate, robust sporodochial conidia, which on average were the largest such conidia occurring among the formally described, clinically relevant species known at that time – namely, *N. falciformis*, *N. keratoplastica* and *N. solani* (Short et al. 2013). Two species described here, *N. gamsii* and *N. suttoniana*, exhibit sporodochial conidia that are somewhat similar in shape and septation. Those of *N. petroliphila*, however, can be distinguished by being much shorter than those of *N. gamsii* and *N. suttoniana* (overall: 44–52.2 µm long), as well as markedly and regularly curved.

Neocosmospora suttoniana Sandoval-Denis & Crous, *sp. nov.* — MycoBank MB822903; Fig. 7

Etymology. In honour and memory of the clinical mycologist Deanna A. Sutton.

Type. USA, Louisiana, from human (CBS H-23224 – holotype; CBS 143214 = NRRL 32858 = FRC S-1423 – culture ex-type).

Sporulation abundant from conidiophores formed directly on the substrate mycelium and less often from sporodochia. *Conidiophores* in the aerial mycelium erect, up to 250 µm tall, commonly solitary and simple, emerging from the agar surface or sporulating at the agar level, rarely 1–3-times branched laterally, bearing terminal monophialides; *phialides* subulate to subcylindrical, smooth- and thin-walled, (6–)23.5–60.5(–63) × (2–)3–3.5(–4) µm, with conspicuous periclinal thickening and a minute, discreet collarette; *conidia* formed on aerial conidiophores, hyaline, obovoid, ellipsoidal, clavate to somewhat cylindrical, straight or curved dorsoventrally, smooth- and thin-walled, 0–2(–3)-septate, (6–)7.5–21(–31) × (2.5–)3–5.5(–7.5) µm, single or grouped in false heads at the tip of monophialides. *Sporodochia* cream to rosy buff coloured, bright, formed scantly and tardily then clustering into dense masses on the surface of carnation leaves. *Conidiophores* in sporodochia 38–58 µm tall, densely packed, cushion-like, irregularly or verticillately branched, with terminal branches bearing 1–3 monophialides; sporodochial phialides subulate to subcylindrical, often curved near the middle portion, (12–)13.5–19(–22.5) × (2.5–)3–4(–5) µm, smooth- and thin-walled, without periclinal thickening and with an inconspicuous apical collarette. Sporodochial *conidia* falcate, widest at the central portion or right above it, gently tapering toward the basal part, robust, somewhat straight on both dorsal and ventral lines; dorsal curvature moderate and often not continuous, being more prominent in the apical and basal thirds; apical cell more or less equally sized or smaller than the adjacent cell, bluntly elongated or distinctly hooked; basal cell somewhat papillate to distinctly notched, (3–)5–6-septate, hyaline, thick- and smooth-walled. Three-septate conidia: 30.5–32.5 × 7–7.5 µm; 4-septate conidia: (49–)50–53.5 × 6–6.5 µm; 5-septate conidia: (30.5–)52–71(–77.5) × (6–)7–8 µm; 6-septate conidia: (75–)77–84.5(–86.5) × (6.5–)7–8 µm; overall (30.5–)50–75(–86.5) × (6–)7–7.5(–8) µm. *Chlamydospores* abundant, spherical to subspherical (4.8–)6–8.5(–9.5) µm diam, solitary or in chains, terminal or intercalary, coarsely roughened to verruculose- and thick-walled.

Culture characteristics — Colonies on PDA growing in the dark with an average radial growth rate of 3.8–5.4 and 5–5.7 mm/d at 21 and 24 °C, respectively, reaching 65–85 mm diam in 7 d at 24 °C. Colony surface straw to olivaceous buff, flat, felty to velvety, aerial mycelium regular, white, formed in radial patches; colony margins regular. Reverse pale luteous to luteous. Pale sulphur yellow to straw diffusible pigments present at 18–36 °C. Colonies on OA and CMA incubated at 24 °C in the dark occupying an entire 9 cm Petri dish in 7 d. Colony colour sulphur yellow to straw, flat, felty to velvety, with rays of abundant aerial mycelium; margins regular. Reverse sulphur yellow to straw, without diffusible pigments.

Cardinal temperatures for growth — Minimum 12 °C, maximum 36 °C, optimal 24–33 °C.

Additional material examined. Gabon, from human nail, *M. Kombila* (CBS 124892). – USA, Massachusetts, from human, *D.A. McGough* (CBS 130178 = NRRL 22608 = UTHSC 93-1547); Georgia, from human blood (CBS 143197 = NRRL 28000); Florida, from human corneal ulcer, *D.A. Sutton* (CBS 143204 = NRRL 32316 = UTHSC 00-264); Florida, from equine eye (CBS 143224 = NRRL 54972 = UTHSC 05-2900).

Notes — Among the newly described species, *N. suttoniana*, previously assigned to clade FSSC 20 of *Neocosmospora* is the taxon that most closely resembles *N. solani* s.str. (Schroers et al. 2016), both species producing mostly 5-septate, robust sporodochial conidia. However, while *N. solani* produces 0–3–5-septate conidia, *N. suttoniana* produces much larger, more frequently septate (up to 6 septa) and more distinctly apically curved conidia, the conidial apex being also more elongated than in *N. solani* and somewhat hooked. In addition, sporodochia in *N. suttoniana* tend to develop belatedly, often after more than 10 d of incubation. Apical curvature is a common feature of sporodochial conidia among the clinically relevant species of *Neocosmospora*; however, it is much more noticeable in *N. suttoniana* and *N. gamsii*. The last two species are also distinguishable morphologically (see notes under *N. gamsii*). Comparable shape and degree of septation of the sporodochial conidia are also recorded for '*Fusarium*' *ensiforme* which, however, produces overall smaller conidia and smooth-walled chlamydospores (Wollenweber & Reinking 1935) vs the verrucose chlamydospores of *N. suttoniana*. Other species producing rough-walled chlamydospores are '*Fusarium' ventricosum* (currently classified as *Rectifusarium ventricosum*, Lombard et al. 2015) and '*F.' solani* var. *minus* (Wollenweber & Reinking 1935), a species rarely reported as an etiologic agent of mycetoma (El-Zaatari & McGinnis 1993). '*Fusarium' solani* var. *minus* forms mostly 3-septate sporodochial conidia (full range 3–5-septate vs (3–)5–6-septate in *N. suttoniana*), smaller (20–41 × 3.5–6 µm vs (30.5–)50–75(–86.5) × (6–)7–7.5(–8) µm in *N. suttoniana*) and more prominently curved conidia than those of *N. suttoniana*. In addition, *N. suttoniana* produces 0–2(–3)-septate aerial conidia (vs 0-septate in *'F.' solani* var. *minus*). *Neocosmospora suttoniana* is an uncommon human pathogenic species, up to now reported from blood and causing eye infections in the USA and Africa (O'Donnell et al. 2008).

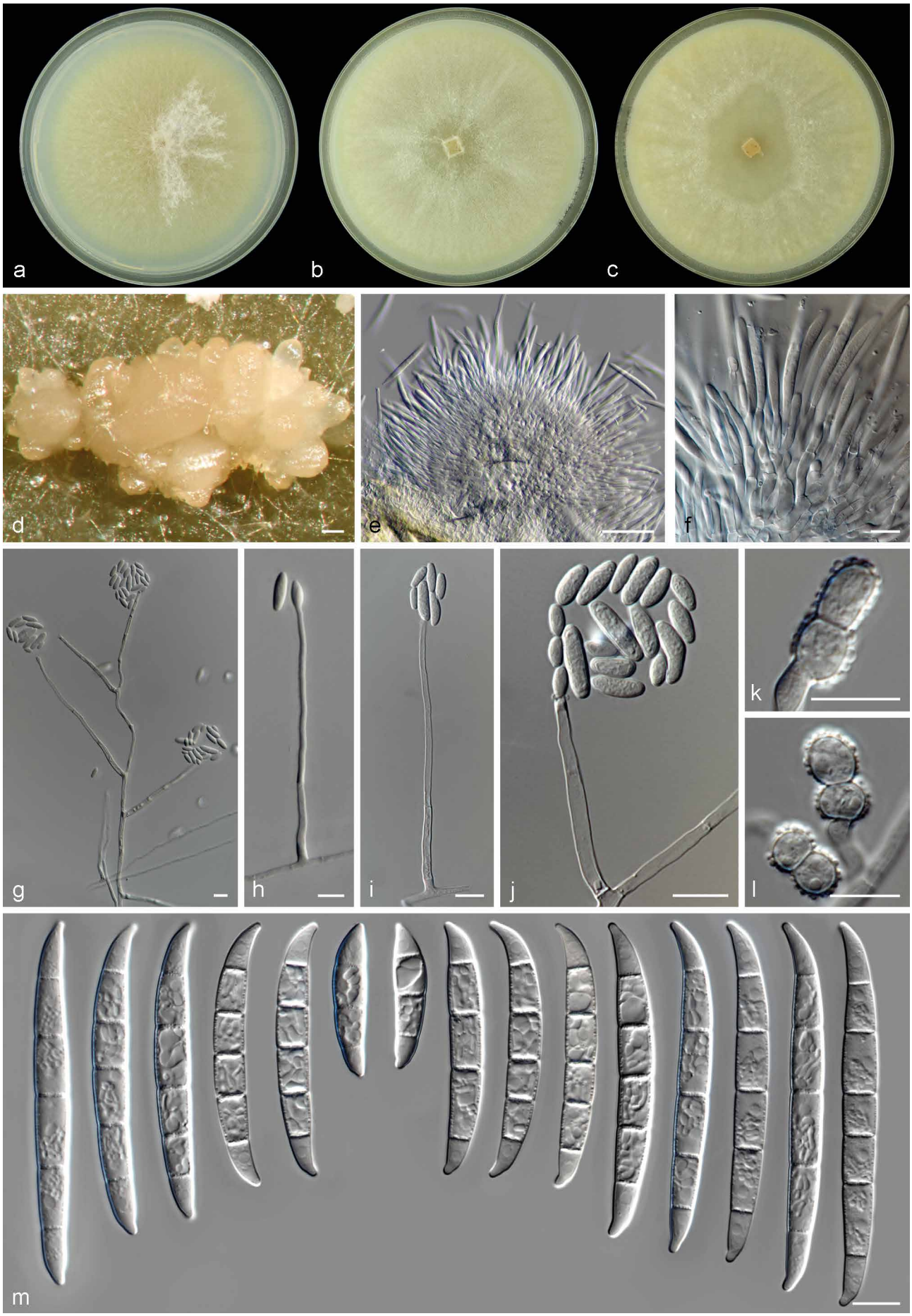

Fig. 7 *Neocosmospora suttoniana*. a. Colony in PDA; b. colony in OA; c. colony in CMA; d. sporodochia formed on the surface of carnation leaves; e–f. sporodochial conidiophores and phialides; g–j. aerial conidiophores, phialides and conidia; k–l. chlamydospores; m. sporodochial conidia. — Scale bars: d–e = 50 µm; all others = 10 µm.

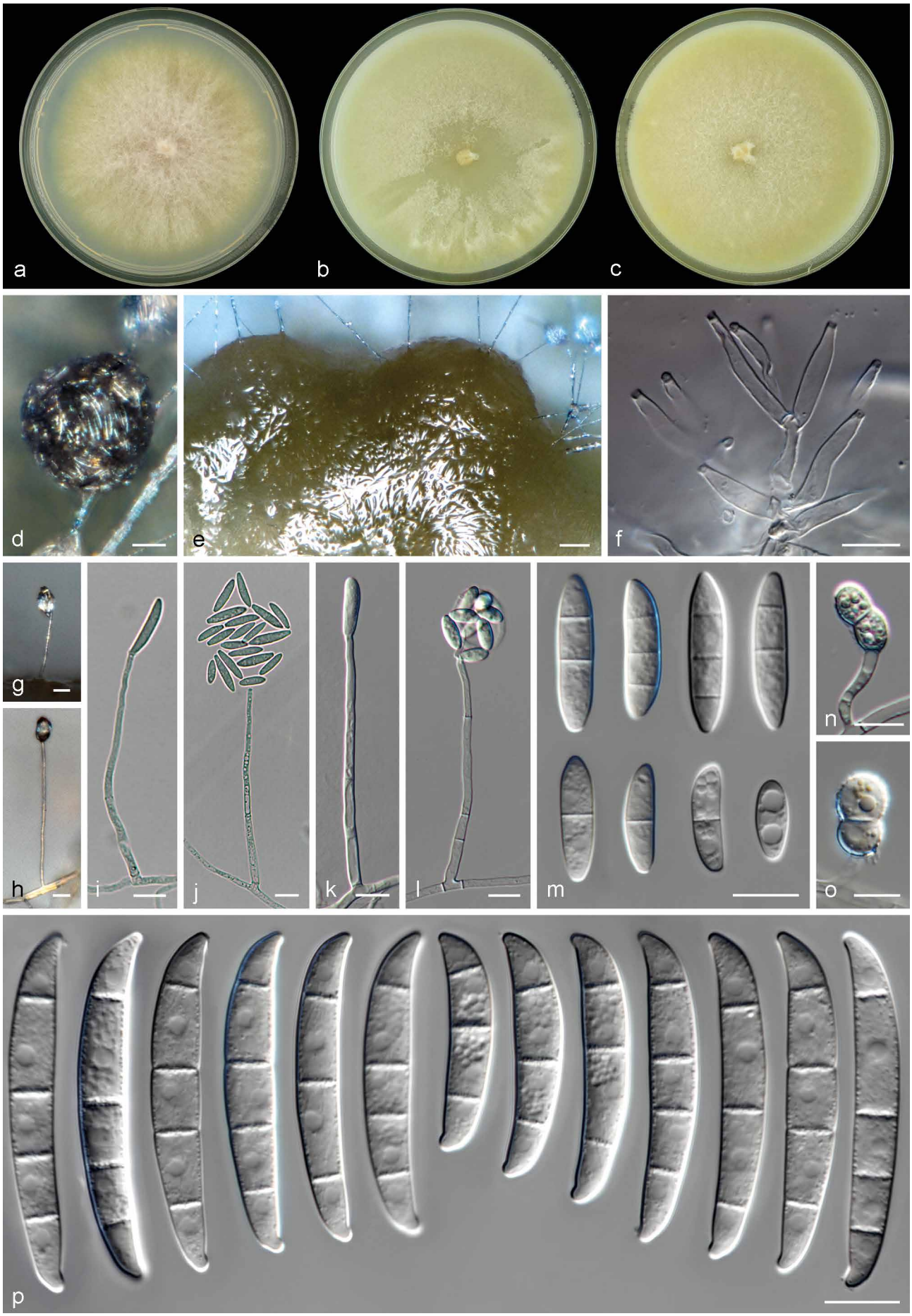

Fig. 8 *Neocosmospora tonkinensis*. a. Colony on PDA; b. colony on OA; c. colony on CMA; d–e. sporodochia formed on the surface of carnation leaves; f. sporodochial conidiophore and phialides; g–l. aerial conidiophores and phialides; m. aerial conidia; n–o. chlamydospores; p. sporodochial conidia. — Scale bars: d–e = 20 µm; all others = 10 µm.

Neocosmospora tonkinensis (Bugnic.) Sandoval-Denis & Crous, *comb. nov.* — MycoBank MB822904; Fig. 8

Basionym. *Cylindrocarpon tonkinense* Bugnic., Encycl. Mycol. 11: 181. 1939.

Synonym. *Fusarium ershadii* Papizadeh et al., Eur. J. Pl. Pathol. doi: 10.1007/s10658-017-1403-6: 5 (2018) (nom. illegit., Art 52.1).

Type. Vietnam, Tonkin, from *Musa sapientum*, 1936, *F. Bugnicourt* No 498 (IMI 113868 – holotype specimen; CBS 115.40 – ex-type culture of *Cylindrocarpon tonkinense*).

Sporulation abundant from sporodochia, and from conidiophores formed on the substrate and aerial mycelium, abundantly produced on hyphal ropes. *Conidiophores* in the aerial mycelium erect, up to 214 µm tall, simple or branched, branching irregular or verticillate, bearing terminal, long monophialides; *phialides* subulate to subcylindrical, straight, smooth- and thin-walled, (42.5–)46.5–63.5 × 3–4(–4.5) µm, periclinal thickening and collarettes inconspicuous; *conidia* formed on aerial conidiophores hyaline, obovate, clavate to ellipsoidal, straight or slightly curved, smooth- and thin-walled, 0–3(–4)-septate, (6–)11–24(–37) × (3.5–)4–6(–7) µm, single or forming small false heads on the tips of monophialides. *Sporodochia* at first citrine to hazel coloured turning dark bluish green, brown, vinaceous to purple slate, formed abundantly and clustering on the surface of carnation leaves and on the agar surface. *Conidiophores* in sporodochia, 22–34.5 µm tall, irregularly or verticillately branched; terminal branches bearing 1–4 monophialides; sporodochial *phialides* subulate, subcylindrical or somewhat ventricose, often swollen in the middle portion, tapering gently toward the apex (15–)16–20(–21) × (2.5–)3–4.5 µm, smooth- and thin-walled, with inconspicuous periclinal thickening, and a minute and short apical collarette. Sporodochial *conidia* wedge-shaped, robust, tapering toward the basal cell, with ventral line gently curved, almost straight between the second septum and the apical cell; dorsal curvature continuous, slightly more pronounced towards the apex; apical cell blunt and typically smaller than the adjacent cell; basal cell blunt to distinctly notched, (1–)3–4(–5)-septate, hyaline, thick- and smooth-walled. One-septate conidia: 47–51 × 6–7.5 µm; 3-septate conidia: (28–)32.5–42.5(–45.5) × (5.5–)6–7.5 µm; 4-septate conidia: (40.5–)43–48(–49) × 6–7.5 µm; 5-septate conidia: (40–)41.5–52 × 6.9–7.3 µm; overall (27.5–)37–48(–50.5) × (5.5–)6–7(–7.5) µm. *Chlamydospores* abundant, spherical to subspherical 6.5–10(–12) µm diam, hyaline to subhyaline, solitary or in pairs, chains or clusters, terminal or intercalary, smooth- and thick-walled.

Culture characteristics — Colonies on PDA growing in the dark with an average radial growth rate of 3.8–5.1 and 4.3–6 mm/d at 21 and 24 °C, respectively, reaching 76–84 mm diam in 7 d at 24 °C. Colony surface buff, honey with sulphur yellow periphery, flat, felty to floccose, radiated with abundant floccose white to yellow aerial mycelium; colony margins regular, fimbriate. Reverse sulphur yellow to brick coloured. Ochreous to fulvous pigments can be produced between 18–24 °C, a bright yellow pigment is formed between 27–30 °C becoming pale yellow to straw at 36 °C. Colonies on OA and CMA incubated at 24 °C in the dark occupying an entire 9 cm Petri dish in 7 d. Colony colour straw, sulphur to pure yellow, flat, felty, velvety to dusty with abundant short aerial mycelium, margins regular. Reverse sulphur yellow with abundant pure yellow diffusible pigment.

Cardinal temperatures for growth — Minimum 9 °C, maximum 36 °C, optimal 27–33 °C.

Additional material examined. Netherlands, Leiden, from human cornea, Oct. 2017, *M.T. van der Beek* (CBS 143038). – USA, Florida, from turtle head lesion (CBS 143208 = NRRL 32755 = FRC S-0452); Ohio, from human cornea (CBS 143217 = NRRL 43811).

Notes — *Neocosmospora tonkinensis*, previously known as FSSC 9, is known to include human pathogens, mostly isolated from corneal specimens (O'Donnell et al. 2008, Muraosa et al. 2017), as well as from animal infections (O'Donnell et al. 2008, 2016). Short et al. (2011) reported also the isolation of this species from water drains in the USA.

As already noted by Summerbell & Schroers (2002), the ex-type strain of *C. tonkinense* (CBS 115.40) clusters within this clade, but is distinctly separated and thus not congeneric with *N. lichenicola* as previously alleged (Hawksworth 1979). However, the former authors prevented any taxonomical changes arguing for a probable strain transposition since tapering, curved conidia were observed. During our examination of the ex-type culture, however, we also found the presence of multiseptate, almost cylindrical aerial conidia with more or less rounded apices. Although the observed conidia were slightly smaller and less septate than those reported in the protologue of *C. tonkinense* (Bugnicourt 1939) (overall from the original description 1–7-septate and 13–45 µm long vs 0–3(–4)-septate and (6–)11–24(–37) µm long in the ex-type); they were more similar in size and shape to those reported for the same strain by Booth (1966), thus a redescription and illustration of the species was provided. The observed differences may easily respond to the different culture conditions employed for the original description of *C. tonkinense* (slices of carrots and potatoes, beans and citrus twigs). Cylindrical aerial conidia of similar characteristic to those reported here were illustrated in the protologue of *Fusarium ershadii*, a superfluous name based on the ex-type culture of *C. tonkinensis* (Papizadeh et al. 2018). Similarly, while sporodochia and falcate multiseptate conidia were not observed in the ex-type, they were readily formed in the clinical isolates examined, phylogenetically shown to be conspecific with *N. tonkinensis*. Sporodochial phialides and conidia strongly resemble those of *N. metavorans*; however, these species are phylogenetically distant.

DISCUSSION

Neocosmospora is perhaps one of the best examples of a fungal genus undergoing fairly rapid speciation (Rossman et al. 1999). Molecular phylogenetic studies have revealed a hidden diversity of phylogenetic species in this genus. There are currently more than 60 recognised genealogically exclusive lineages, many of them showing pathogenic potential against plants, humans and diverse animals (O'Donnell 2000, Summerbell & Schroers 2002, O'Donnell et al. 2008, 2012, 2016, Sandoval-Denis et al. 2018). Our phylogenetic results were highly consistent with previous phylogenetic analyses (O'Donnell et al. 2008, 2016, Gräfenhan et al. 2011, Schroers et al. 2011, Lombard et al. 2015). *Neocosmospora* was found to be monophyletic, containing a surprisingly high diversity, with many species still needing a proper study and formal descriptions.

Achieving morphological species delimitation and identification in *Neocosmospora* and related genera is a difficult task, especially among human pathogenic species. Although morphological observations proved to be of great value when the appropriate morphological traits were evaluated under standardised culture conditions, we found notable interspecific differences in conidial dimensions, septation and shape for both aerial and sporodochial conidia. These differences, coupled with other features such as the chlamydospore surface texture, the overall cultural growth characteristics and the host of origin, can be of great value for presumptive identification of human and animal pathogenic species. However, considering that these organisms are highly variable in culture, molecular tools should always be applied, in order to ensure correct identification of the involved

species. The general recommendation for clinical microbiologists is to assess species level identification of these pathogens using *EF-1α* and *RPB2* sequences, compared with curated reference sequences deposited in recognised databases as FUSARIUM-ID (http://isolate.fusariumdb.org, Geiser et al. 2004) and Fusarium MLST (http://www.westerdijkinstitute.nl/Fusarium/) (O'Donnell et al. 2015, 2016). As also confirmed here, these two loci have high resolving power and allowed for a correct delimitation of the clinically relevant clades. This was especially true of *RPB2*, the only gene in our dataset able to identify all the pathogenic species with great certainty.

Sexual morphs are not usually found in culture. Only a third of the known *Neocosmospora* species, mostly plant-pathogenic taxa, have a known sexual morph (O'Donnell 2000, O'Donnell et al. 2008, Coleman 2016). Among the clinically relevant species, only *N. keratoplastica*, *N. petroliphila*, and an uncommon species, *N. pseudensiformis*, have been described with a sexual morph (Nalim et al. 2011, Short et al. 2013). Here, a sexual morph was described for *N. gamsii*. It was observed only in the ex-type strain and was produced homothallically, after prolonged incubation under standard culture conditions. However, given the infrequent occurrence of sexual structures in *Neocosmospora*, these features are not reliable in species delimitation (O'Donnell 2000).

Neocosmospora catenata was described here without sporodochial conidia, an important morphological feature for generic and, to some extent, specific classification. The lack of macroconidia is not uncommon in fresh *Neocosmospora* isolates, but in most cases, the production of such structures can be induced using carnation leaf agar or exposure to UV light; these techniques were ineffective in *N. catenata*. A failure to produce macroconidia should not be regarded as a potential differential character (Leslie & Summerell 2006). Caution is particularly suggested by the knowledge that other *Neocosmospora* species were originally based on concepts derived from isolates failing to produce macroconidia. For instance, *N. falciformis*, one the most prevalent fusarial human pathogens (O'Donnell et al. 2008, Guarro 2013) is based on *Cephalosporium falciforme*, originally described as producing only microconidia grouped in false heads on the tip of thin and elongated monophialides (Carrión 1951). This species was transferred to the genus *Acremonium* by Gams (1971), partly because of this morphology but also because the human-host-adapted ex-type isolate had a growth rate that fell below Gams' recognition standard for distinguishing *Fusarium* isolates. Molecular data, however, showed this species to cluster within the '*Fusarium*' *solani* species complex, now *Neocosmospora* (Summerbell & Schroers 2002). Many fresh isolations of this species have later evidenced the production of distinctive multiseptate conidia, confirming its affinity with *Neocosmospora* (Edupuganti et al. 2011, Short et al. 2013, Chehri et al. 2015). Similarly, the recently described *N. metavorans* was characterised as lacking sporodochial conidia (Al-Hatmi et al. 2018). However, sporodochial conidia were readily produced by the large set of human-pathogenic isolates studied here, and the species was appropriately redescribed and illustrated.

The highly relevant clade FSSC 12, although included in our phylogenetic analyses, was not linked to a Latin binomial in this study. Members of this clade have been thoroughly evaluated and a formal description is being prepared in a different study (Geiser pers. comm.). Phylospecies FSSC 12 is known to cause lethal animal infections spanning a wide spectrum of host species, particularly aquatic animals held in captivity. Species affected include American lobster (*Hamarus americanus*) (Lightner & Fontaine 1975), antler crab (*Manucomplanus varians*), honeycomb cowfish (*Acanthostracion polygonius*), horseshoe crab, sea turtle (*Lepidochelys kempii*) (O'Donnell et al. 2016), kuruma prawn (*Penaeus japonicus*) (Hatai et al. 1978), lined sea horse (*Hippocampus erectus*) (Salter et al. 2012), stingray (*Taeniura melanopsila*), scalloped hammerhead shark (*Sphyrna lewini*) (Fernando et al. 2015) and treefish (*Sebastes serriceps*) (O'Donnell et al. 2008). The species has also been found in water and sand from human-made aquatic habitats (O'Donnell et al. 2008).

The authors of this paper are aware that the generic placement of these taxa is controversial since, to date, two opposite views exist. However, while some researchers have indicated a preference for conserving the generic name *Fusarium* (= *Gibberella*) in a broad sense, to also include the genus *Neocosmospora*, no formal decision has yet been made to conserve the broad definition of *Fusarium* sensu Geiser et al. (2013), against morphologically and phylogenetically supported genera such as *Neocosmospora* (Gräfenhan et al. 2011, Schroers et al. 2011, Lombard et al. 2015). The concept espoused by Geiser et al. (2013) is broad and polyphyletic, encompassing an artificial arrangement of many distinct clades/genera with clearly different sexual morphologies. We have employed a taxonomical approach that, in our perspective is based on a sound and more natural classification, based not only in molecular phylogenetic exclusiveness, but also considering holomorphic morphological characters. Clinical microbiologists are encouraged to use up-to-date taxonomy and nomenclature for this fungal group and apply the generic name *Neocosmospora*, which embraces species demonstrated by substantial morphological and molecular evidence not to be congeneric with their closest relatives in *Fusarium* (Rossman et al. 1999, Gräfenhan et al. 2011, Schroers et al. 2011, Lombard et al. 2015, Sandoval-Denis et al. 2018).

Acknowledgements We thank Todd J. Ward and David Labeda (Agricultural Research Service, US Department of Agriculture, Peoria, Illinois) for providing strains, and Kerry O'Donnell (Agricultural Research Service, US Department of Agriculture, Peoria, Illinois) for kindly sharing DNA sequence alignments used in this study, including unpublished material. Konstanze Bensch, curator of Mycobank, is thanked for her help discussing nomenclatural problems. Abdullah Al-Hatmi (Westerdijk Fungal Biodiversity Institute, Utrecht, The Netherlands) for sharing valuable information regarding *N. metavorans*, and Trix Merkx (Westerdijk Fungal Biodiversity Institute, Utrecht, The Netherlands) for helping with culture deposits.

REFERENCES

Al-Hatmi AMS, Ahmed SA, Van Diepeningen AD, et al. 2018. Fusarium metavorans sp. nov.: the frequent opportunist 'FSSC6'. Medical Mycology 56: S144–S152.

Alastruey-Izquierdo A, Cuenca-Estrella M, Monzón A, et al. 2008. Antifungal susceptibility profile of clinical Fusarium spp. isolates identified by molecular methods. Journal of Antimicrobial Chemotherapy 61: 805–809.

Amby DB, Thuy TTT, Ho DB, et al. 2015. First report of Fusarium lichenicola as a causal agent of fruit rot in pomelo (Citrus maxima). Plant Disease 99: 1278.

Aoki T, O'Donnell K, Homma Y, et al. 2003. Sudden-death syndrome of soybean is caused by two morphologically and phylogenetically distinct species within the Fusarium solani species complex – F. virguliforme in North America and F. tucumaniae in South America. Mycologia 95: 660–684.

Aoki T, O'Donnell K, Scandiani MM. 2005. Sudden death syndrome of soybean in South America is caused by four species of Fusarium: Fusarium brasiliense sp. nov., F. cuneirostrum sp. nov., F. tucumaniae and F. virguliforme. Mycologia 46: 162–183.

Aoki T, Smith JA, Mount LL, et al. 2013. Fusarium torreyae sp. nov., a pathogen causing canker disease of Florida torreya (Torreya taxifolia), a critically endangered conifer restricted to northern Florida and southwestern Georgia. Mycologia 105: 312–319.

Araujo R, Oliveira M, Amorim A, et al. 2015. Unpredictable susceptibility of emerging clinical moulds to tri-azoles: review of the literature and upcoming challenges for mould identification. European Journal of Clinical Microbiology and Infectious Diseases 34: 1289–1301.

Azor M, Gené J, Cano J, et al. 2007. Universal in vitro antifungal resistance of genetic clades of the Fusarium solani species complex. Antimicrobial Agents and Chemotherapy 51: 1500–1503.
Bachmeyer C. 2007. Deep cutaneous infection by Fusarium solani in a healthy child. Journal of the American Academy of Dermatology 57: 1095–1096.
Booth C. 1966. The genus Cylindrocarpon. Mycological Papers 104: 1–56.
Bugnicourt F. 1939. Les Fusarium et Cylindrocarpon de l'Indochine. Encyclopédie Mycologique 11: 1–206.
Carrión AL. 1951. Cephalosporium falciforme sp. nov., a new etiologic agent of maduromycosis. Mycologia 43: 522–523.
Champa H, Sreeshma P, Yegneswaran Prakash P, et al. 2013. Cutaneous infection with Cylindrocarpon lichenicola. Medical Mycology Case Reports 2: 55–58.
Chang DC, Grant GB, O'Donnell K, et al. 2006. Multistate outbreak of Fusarium keratitis associated with use of a contact lens solution. Journal of the American Medical Association 296: 953–963.
Chazan B, Colodner R, Polacheck I, et al. 2004. Mycetoma of the foot caused by Cylindrocarpon lichenicola in an immunocompetent traveller. Journal of Travel Medicine 11: 331–332.
Chehri K, Salleh B, Zakaria L. 2015. Morphological and phylogenetic analysis of Fusarium solani species complex in Malaysia. Microbial Ecology 69: 457–471.
Chen KL, Kirschner R. 2017. Fungi from leaves of lotus (Nelumbo nucifera). Mycological Progress 17: 275–293. doi: https://doi.org/10.1007/s11557-017-1324-y
Coleman JJ. 2016. The Fusarium solani species complex: ubiquitous pathogens of agricultural importance. Molecular Plant Pathology 17: 146–158.
Crous PW, Verkley GJM, Groenewald JZ, et al. (eds). 2009. Fungal biodiversity. CBS Laboratory Manual Series 1. CBS-KNAW Fungal Biodiversity Centre, Utrecht, The Netherlands.
De Hoog GS, Guarro J, Gené J, et al. 2000. Atlas of clinical fungi, 2nd ed. Centraalbureau voor Schimmelcultures, Utrecht, The Netherlands.
Dignani MC, Anaissie E. 2004. Human fusariosis. Clinical Microbiology and Infection 10: 67–75.
Domsch KH, Gams W, Anderson TH. 2007. Compendium of soil fungi. 2nd edn. IHW Verlag, Eching, Germany.
Edupuganti S, Rouphael N, Mehta A, et al. 2011. Fusarium falciforme vertebral abscess and osteomyelitis: case report and molecular classification. Journal of Clinical Microbiology 49: 2350–2353.
El-Zaatari M, McGinnis MR. 1993. Mycotic mycetoma. In: Murphy JW, Friedman H, Bendinelli M (eds), Fungal infections and immune responses: 325–334. Plenum Press, USA.
Ersal T, Al-Hatmi AS, Cilo BD, et al. 2015. Fatal disseminated infection with Fusarium petroliphilum. Mycopathologia 179: 119–124.
Espinel-Ingroff A, Colombo AL, Cordoba S, et al. 2016. International evaluation of MIC distributions and epidemiological cutoff value (ECV) definitions for Fusarium species identified by molecular methods for the CLSI broth microdilution method. Antimicrobial Agents and Chemotherapy 60: 1079–1084.
Farr DF, Rossman AY. 2017. Fungal databases, U.S. National Fungus Collections, ARS, USDA. Retrieved July 25, 2017, from https://nt.ars-grin.gov/fungaldatabases/.
Fernando N, Hui SW, Tsang CC, et al. 2015. Fatal Fusarium solani species complex infections in elasmobranchs: the first case report for black spotted stingray (Taeniura melanopsila) and a literature review. Mycoses 58: 422–431.
Fisher NL, Burguess LW, Toussoun TA, et al. 1982. Carnation leaves as a substrate and for preserving cultures of Fusarium species. Phytopathology 72: 151–153.
Gams W. 1971. Cephalosporium-artige Schimmelpilze (Hyphomycetes). Fischer, Germany.
Garcia RR, Min Z, Narasimhan S, et al. 2015. Fusarium brain abscess: case report and literature review. Mycoses 58: 22–26.
Geiser DM, Aoki T, Bacon CW, et al. 2013. One fungus, one name: defining the genus Fusarium in a scientifically robust way that preserves longstanding use. Phytopathology 103: 400–408.
Geiser DM, Jiménez-Gasco M, Kang S, et al. 2004. FUSARIUM-ID v.1.0: A DNA sequence database for identifying Fusarium. European Journal of Plant Pathology 110: 473–479.
Ghannoum MA, Hajjeh RA, Scher R, et al. 2000. A large-scale North American study of fungal isolates from nails: the frequency of onychomycosis, fungal distribution, and antifungal susceptibility patterns. Journal of the American Academy of Dermatology 43: 641–648.
Godoy P, Cano J, Gené J, et al. 2004. Genotyping of 44 isolates of Fusarium solani, the main agent of fungal keratitis in Brazil. Journal of Clinical Microbiology 42: 4494–4497.
Gräfenhan T, Schroers HJ, Nirenberg HI, et al. 2011. An overview of the taxonomy, phylogeny, and typification of nectriaceous fungi in Cosmospora, Acremonium, Fusarium, Stilbella, and Volutella. Studies in Mycology 68: 79–113.
Guarro J. 2013. Fusariosis, a complex infection caused by a high diversity of fungal species refractory to treatment. European Journal of Clinical Microbiology and Infectious Diseases 32: 1491–1500.
Guevara-Suarez M, Cano-Lira JF, De García MC, et al. 2016. Genotyping of Fusarium isolates from onychomycoses in Colombia: detection of two new species within the Fusarium solani species complex and in vitro antifungal susceptibility testing. Mycopathologia 181: 165–174.
Hatai K, Furuya K, Egusa S. 1978. Studies on the pathogenic fungus associated with black gill disease of kuruma prawn, Penaeus japonicas. I. Isolation and identification of the BG-Fusarium. Fish Pathology 12: 219–224.
Hawksworth DL. 1979. The lichenicolous hyphomycetes. Bulletin of the British Museum (Natural History), Botany 6: 183–300.
Herr JR, Scully ED, Geib SM, et al. 2016. Genome sequence of Fusarium isolate MYA-4552 from the midgut of Anoplophora glabripennis, an invasive, wood-boring beetle. Genome Announcements 4: e00544-16.
Hiebert RM, Welliver RC, Yu Z. 2016. Fusarium osteomyelitis in a patient with Pearson syndrome: case report and review of the literature. Open Forum Infectious Diseases 3: ofw183.
Huelsenbeck JP, Ronquist F. 2001. MrBayes: Bayesian inference of phylogeny. Bioinformatics 17: 754–755.
Katoh K, Standley DM. 2013. MAFFT multiple sequence alignment software v. 7: improvements in performance and usability. Molecular Biology and Evolution 30: 772–780.
Kumar S, Stecher G, Tamura K. 2016. MEGA7: Molecular Evolutionary Genetics Analysis version 7.0 for bigger datasets. Molecular Biology and Evolution 33: 1870–1874.
Lass-Flörl C. 2009. The changing face of epidemiology of invasive fungal disease in Europe. Mycoses 52: 197–205.
Leslie JF, Summerell BA. 2006. The Fusarium laboratory manual. Blackwell Publishing, Ames.
Li W, Cowley A, Uludag M, et al. 2015. The EMBL-EBI bioinformatics web and programmatic tools framework. Nucleic Acids Research 43: W580–W584.
Lightner DV, Fontaine CT. 1975. A mycosis of the American lobster, Hamarus americanus caused by Fusarium sp. Journal of Invertebrate Pathology 25: 239–245.
Liu D. 2011. Cylindrocarpon. In: Liu D (ed), Molecular detection of human fungal pathogens: 411–415. CRC Press, USA.
Liu YJ, Whelen S, Hall BD. 1999. Phylogenetic relationships among ascomycetes: evidence from an RNA polymerse II subunit. Molecular Biology and Evolution 16: 1799–1808.
Lombard L, Van der Merwe NA, Groenewald JZ, et al. 2015. Generic concepts in Nectriaceae. Studies in Mycology 80: 189–245.
Mason-Gamer R, Kellogg E. 1996. Testing for phylogenetic conflict among molecular data sets in the tribe Triticeae (Gramineae). Systematic Biology 45: 524–545.
Mehl HL, Epstein L. 2008. Sewage and community shower drains are environmental reservoirs of Fusarium solani species complex group 1, a human and plant pathogen. Environmental Microbiology 10: 219–227.
Melo MP, Beserra Jr JEA, Matos KS, et al. 2016. First report of a new lineage in the Fusarium solani species complex causing root rot on sunn hemp in Brazil. Plant Disease 100: 1784.
Miller MA, Pfeiffer W, Schwartz T. 2012. The CIPRES science gateway: enabling high-impact science for phylogenetics researchers with limited resources. In: Proceedings of the 1st Conference of the Extreme Science and Engineering Discovery Environment: Bridging from the extreme to the campus and beyond: 1–8. Association for Computing Machinery, USA.
Muraosa Y, Oguchi M, Yahiro M, et al. 2017. Epidemiological study of Fusarium species causing invasive and superficial fusariosis in Japan. Medical Mycology Journal 58: E5–E13.
Nakamura Y, Xu X, Saito Y, et al. 2007. Deep cutaneous infection by Fusarium solani in a healthy child: successful treatment with local heat therapy. Journal of the American Academy of Dermatology 56: 873–877.
Nalim FA, Samuels GJ, Wijesundera RL, et al. 2011. New species from the Fusarium solani species complex derived from perithecia and soil in the old world tropics. Mycologia 103: 1302–1330.
Nirenberg HI. 1976. Untersuchungen über die morphologische und biologische Differenzierung in der Fusarium-Sektion Liseola. Mitteilungen der Biologischen Bundesanstalt für Land- und Forstwirtschaft Berlin-Dahlem 169: 1–117.
Nylander JAA. 2004. MrModeltest v2. Program distributed by the author. Evolutionary Biology Centre, Uppsala University.
O'Donnell K. 2000. Molecular phylogeny of the Nectria haematococca–Fusarium solani species complex. Mycologia 92: 919–938.

O'Donnell K, Humber RA, Geiser DM, et al. 2012. Phylogenetic diversity of insecticolous fusaria inferred from multilocus DNA sequence data and their molecular identification via FUSARIUM-ID and Fusarium MLST. Mycologia 104: 427–445.

O'Donnell K, Kistler HC, Cigelnik E, et al. 1998. Multiple evolutionary origins of the fungus causing Panama disease of banana: concordant evidence from nuclear and mitochondrial gene genealogies. Proceedings of the National Academy of Sciences of the United States of America 95: 2044–2049.

O'Donnell K, Sarver BAJ, Brandt M, et al. 2007. Phylogenetic diversity and microsphere array-based genotyping of human pathogenic fusaria, including isolates from the multistate contact lens-associated U.S. keratitis outbreaks of 2005 and 2006. Journal of Clinical Microbiology 45: 2235–2248.

O'Donnell K, Sutton DA, Fothergill A, et al. 2008. Molecular phylogenetic diversity, multilocus haplotype nomenclature, and in vitro antifungal resistance within the Fusarium solani species complex. Journal of Clinical Microbiology 46: 2477–2490.

O'Donnell K, Sutton DA, Rinaldi MG, et al. 2010. Internet-accessible DNA sequence database for identifying fusaria from human and animal infections. Journal of Clinical Microbiology 48: 3708–3718.

O'Donnell K, Sutton DA, Wiederhold N, et al. 2016. Veterinary fusarioses within the United States. Journal of Clinical Microbiology 54: 2813–2819.

O'Donnell K, Ward TJ, Robert VARG, et al. 2015. DNA sequence-based identification of Fusarium: Current status and future directions. Phytoparasitica 43: 583–595.

Papizadeh M, Van Diepeningen AD, Zamanizadeh HR, et al. 2018. Fusarium ershadii sp. nov., a pathogen on Asparagus officinalis and Musa acuminata. European Journal of Plant Pathology. In press. doi: https://doi.org/10.1007/s10658-017-1403-6.

Petersen RH. 1959. A new species of Mastigosporium from tropical soil. Mycologia 51: 729–733.

Rodríguez-Villalobos H, Georgala A, Beguin H, et al. 2003. Disseminated infection due to Cylindrocarpon (Fusarium) lichenicola in a neutropenic patient with acute leukaemia: Report of a case and review of the literature. European Journal of Clinical Microbiology and Infectious Diseases 22: 62–65.

Romberg MK, Davis RM. 2007. Host range and phylogeny of Fusarium solani f. sp. eumartii from potato and tomato in California. Plant Disease 91: 585–592. doi: https://doi.org/10.1094/PDIS-91-5-0585.

Ronquist F, Huelsenbeck JP. 2003. MrBayes 3: Bayesian phylogenetic inference under mixed models. Bioinformatics 19: 1572–1574.

Rossman AY, Samuels GJ, Rogerson CT, et al. 1999. Genera of Bionectriaceae, Hypocreaceae, and Nectriaceae (Hypocreales, Ascomycetes). Studies in Mycology 42: 1–248.

Salter CE, O'Donnell K, Sutton DA, et al. 2012. Dermatitis and systemic mycosis in lined seahorses Hippocampus erectus associated with a marine-adapted Fusarium solani species complex pathogen. Diseases of Aquatic Organisms 101: 23–31.

Sandoval-Denis M, Guarnaccia V, Polizzi G, et al. 2018. Symptomatic Citrus trees reveal a new pathogenic lineage in Fusarium and two new Neocosmospora species. Persoonia 40: 1–25.

Sarmiento-Ramírez JM, Abella-Pérez E, Phillott AD, et al. 2014. Global distribution of two fungal pathogens threatening endangered sea turtles. PLoS ONE 9: e85853.

Sarmiento-Ramírez JM, Sim J, Van West P, et al. 2017. Isolation of fungal pathogens from eggs of the endangered sea turtle species Chelonia mydas in Ascension Island. Journal of the Marine Biological Association of the United Kingdom 97: 661–667.

Scheel CM, Hurst SF, Barreiros G, et al. 2013. Molecular analyses of Fusarium isolates recovered from a cluster of invasive mold infections in a Brazilian hospital. BMC Infectious Diseases 13: 49.

Scher RK, Rich P, Pariser D, et al. 2013. The epidemiology, etiology, and pathophysiology of onychomycosis. Seminars in Cutaneous Medicine and Surgery 32: S2–S4.

Schroers HJ, Gräfenhan T, Nirenberg HI, et al. 2011. A revision of Cyanonectria and Geejayessia gen. nov., and related species with Fusarium-like anamorphs. Studies in Mycology 68: 115–138.

Schroers HJ, Samuels GJ, Zhang N, et al. 2016. Epitypification of Fusisporium (Fusarium) solani and its assignment to a common phylogenetic species in the Fusarium solani species complex. Mycologia 108: 806–819.

Shaffer JP, U'Ren JM, Gallery RE, et al. 2017. An endohyphal bacterium (Chitinophaga, bacteroidetes) alters carbon source use by Fusarium keratoplasticum (F. solani species complex, Nectriaceae). Frontiers in Microbiology 8: 350.

Shaw DE. 1984. Microorganisms in Papua New Guinea. Department of Primary Industry and Resources Bulletin 33: 1–344.

Short DPG, O'Donnell K, Geiser DM. 2014. Clonality, recombination, and hybridization in the plumbing-inhabiting human pathogen Fusarium keratoplasticum inferred from multilocus sequence typing. BMC Evolutionary Biology 14: 91.

Short DPG, O'Donnell K, Thrane U, et al. 2013. Phylogenetic relationships among members of the Fusarium solani species complex in human infections and the descriptions of F. keratoplasticum sp. nov. and F. petroliphilum stat. nov. Fungal Genetics and Biology 53: 59–70.

Short DPG, O'Donnell K, Zhang N, et al. 2011. Widespread occurrence of diverse human pathogenic types of the fungus Fusarium detected in plumbing drains. Journal of Clinical Microbiology 49: 4264–4272.

Shukla PK, Kumar M, Keshava GB. 2008. Mycotic keratitis: an overview of diagnosis and therapy. Mycoses 51: 183–199.

Slavin M, Van Hal S, Sorrell TC, et al. 2015. Invasive infections due to filamentous fungi other than Aspergillus: epidemiology and determinants of mortality. Clinical Microbiology and Infection 21: 490.e1–490.e10.

Snyder WC, Hansen HN. 1947. Advantages of natural media and environments in the culture of fungi. Phytopathology 37: 420–421.

Stamatakis A. 2014. RAxML version 8: a tool for phylogenetic analysis and post-analysis of large phylogenies. Bioinformatics 30: 1312–1313.

Sugiura Y, Sugita-Konishi Y, Kumagai S, et al. 2003. Experimental murine hyalohyphomycosis with soil-derived isolates of Fusarium solani. Medical Mycology 41: 241–247.

Summerbell RC, Schroers HJ. 2002. Analysis of phylogenetic relationship of Cylindrocarpon lichenicola and Acremonium falciforme to the Fusarium solani species complex and a review of similarities in the spectrum of opportunistic infections caused by these fungi. Journal of Clinical Microbiology 40: 2866–2875.

Sung GH, Sung JM, Hywel-Jones NL, et al. 2007. A multi-gene phylogeny of Clavicipitaceae (Ascomycota, Fungi): Identification of localized incongruence using a combinational bootstrap approach. Molecular Phylogenetics and Evolution 44: 1204–1223.

Swofford DL. 2002. PAUP*. Phylogenetic Analysis Using Parsimony (*and other methods). Version 4. Sinauer Associates, Sunderland, Massachusetts, USA.

Taj-Aldeen SJ, Salah H, Al-Hatmi AM, et al. 2016. In vitro resistance of clinical Fusarium species to amphotericin B and voriconazole using the EUCAST antifungal susceptibility method. Diagnostic Microbiology and Infectious Disease 85: 438–443.

Torres HA, Kontoyiannis DP. 2011. Hyalohyphomycoses (hyaline moulds). In: Kauffman C, Pappas PG, Sobel JD (eds), Essentials of clinical mycology, 2nd ed.: 281–304. Springer, USA.

Tortorano AM, Prigitano A, Dho G, et al. 2008. Species distribution and in vitro antifungal susceptibility patterns of 75 clinical isolates of Fusarium spp. from northern Italy. Antimicrobial Agents and Chemotherapy 52: 2683–2685.

Toussoun TA, Snyder WC. 1961. The pathogenicity, distribution, and control of two races of Fusarium (Hypomyces) solani f. cucurbitae. Phytopathology 51: 17–22.

Usharani P, Ramarao P. 1981. Corm rot of Colocasia esculenta caused by Cylindrocarpon lichenicola. Indian Phytopathology 34: 381–382.

Vilgalys R, Hester M. 1990. Rapid genetic identification and mapping of enzymatically amplified ribosomal DNA from several Cryptococcus species. Journal of Bacteriology 172: 4238–4246.

Vilgalys R, Sun BL. 1994. Ancient and recent patterns of geographic speciation in the oyster mushroom Pleurotus revealed by phylogenetic analysis of ribosomal DNA sequences. Proceedings of the National Academy of Sciences of the United States of America 91: 4599–4603.

White TJ, Bruns T, Lee SB, et al. 1990. Amplification and direct sequencing of fungal ribosomal RNA genes for phylogenetics. In: Innis MA, Gelfand DH, Sninsky JJ, et al. (eds), PCR protocols: a guide to methods and applications: 315–322. Academic Press, USA.

Wiens JJ. 1998. Testing phylogenetic methods with tree congruence: phylogenetic analysis of polymorphic morphological characters in phrynosomatid lizards. Systematic Biology 47: 427–444.

Wollenweber HW. 1916. Fusaria Autographice Delineata 1: 1–509.

Wollenweber HW, Reinking OA. 1935. Die Fusarien, ihre Beschreibung, Schadwirkung und Bekämpfung. Parey, Berlin.

Zhang N, O'Donnell K, Sutton DA, et al. 2006. Members of the Fusarium solani species complex that cause infections in both humans and plants are common in the environment. Journal of Clinical Microbiology 44: 2186–2190.